https://doi.org/10.1016/j.agrformet.2021.108723

Agricultural and Forest Meteorology 312 (2022) 108723

Contents lists available at ScienceDirect

Agricultural and Forest Meteorology

journal homepage: www.elsevier.com/locate/agrformet

Characteristics of lightning-caused wildfires in central Brazil in relation to cloud-ground and dry lightning

Vanúcia Schumacher [a,*,#], Alberto Setzer [a], Marcelo M.F. Saba [a], Kleber P. Naccarato [a], Enrique Mattos [b], Flávio Justino [c]

[a] National Institute for Space Research (INPE), São José dos Campos, SP, Brazil
[b] Federal University of Itajubá, Natural Resources Institute, Itajubá, MG, Brazil
[c] Federal University of Viçosa, Department of Agricultural Engineering, Viçosa, MG, Brazil

ARTICLE INFO

Keywords:
Natural wildfires
Remote sensing
Lightning
Dry lightning

ABSTRACT

Lightning ignition is the major cause of natural wildfires in several regions worldwide. Determining if wildfires in remote uncontrolled areas result from natural lightning as opposed to anthropic action is a relevant and yet-unsolved challenge for large regions of the planet, with scientific and management implications ranging from environmental conservation to mitigation of climate-related emissions of gases and aerosols. Brazil is the country with one of the highest occurrences of lightning (50 to 100 million/year) and which is also subject to numerous and vast wildfires (up to ~600 × 10^3 km^2/year) affecting all its biomes. To quantify natural fires we combined cloud-to-ground (CG) lightning and CG dry-lightning (CGDL) detected by a ground network, with fire pixels mapped by satellite remote sensing (AQUA, S-NPP and NOAA-20) over ~1,8 × 10^6 km^2 in Central Brazil, between 2015 to 2019. Lightning ignition candidates were selected based on the distance between fires and lightning in time and space. The selected cases were investigated according to annual and monthly distributions in space and time, to local weather at the time of occurrence and, electrical characteristics related to ignition. Space-time distributions of CG lightning, CGDL and of active fires were also analyzed. Results showed that the CGDLs pattern is not different from that of the overall CG lightning, with both presenting similar kernel density, polarity and peak current. The lightning candidates indicated predominance of negative polarity and peak current frequency below 20 kA. In this range, average values for weather conditions for CG lightning matched to fires (CGDL matched to fires) had: precipitation 6 mm (< 1 mm), relative humidity 57 % (48 %), and temperature ~30°C and wind speed of ~ 2 $m.s^{-1}$ for both. The results showed that satellite detection of active fires is a useful tool to identify lightning-induced wildfires.

1. Introduction

Wildfires are interconnected with ecosystems dynamics, particularly in fire-prone contexts by providing beneficial effects in rejuvenating vegetation, recycling soils nutrients, controlling invasive species and pathogens, among others ecological implications (Bond et al., 2005; Bowman et al., 2009; IPCC, 2014). However, human-induced land changes and ongoing climate changes in the last decades have altered natural fire regimes leading to increased frequency and wildfire duration (Westerling et al., 2006; Jolly et al., 2015; Werf et al., 2017; Rodman et al., 2019; Gannom and Steinberg 2021). On a broader scale, large-scale wildfires pose a risk to human health and lives, with economic and social adverse impacts, and also interfering on climate and forest ecosystems.

Most wildfire occurrences are related to human-environment interactions and depend on several factors such as: fuel load, vegetation type, topographic conditions, human actions, source of ignition and weather patterns (Schoennagel et al., 2004; Ye et al., 2017). As discussed by (Silva et al., 2021) and Justino et al., (2021), wildfire danger and occurrence may not be directly linked to atmospheric conditions on the day of a wildfire event. Environmental susceptibility to fires can respond to periods of dry spells, even with short-interval precipitation events, in consonance with high temperatures and vapor pressure deficit. Additionally, wildfire risk has been intensively studied in terms of its

* Corresponding author.
E-mail address: vanucia-schumacher@hotmail.com (V. Schumacher).
https://orcid.org/0000-0003-1753-567X

https://doi.org/10.1016/j.agrformet.2021.108723
Received 14 June 2021; Received in revised form 15 October 2021; Accepted 10 November 2021

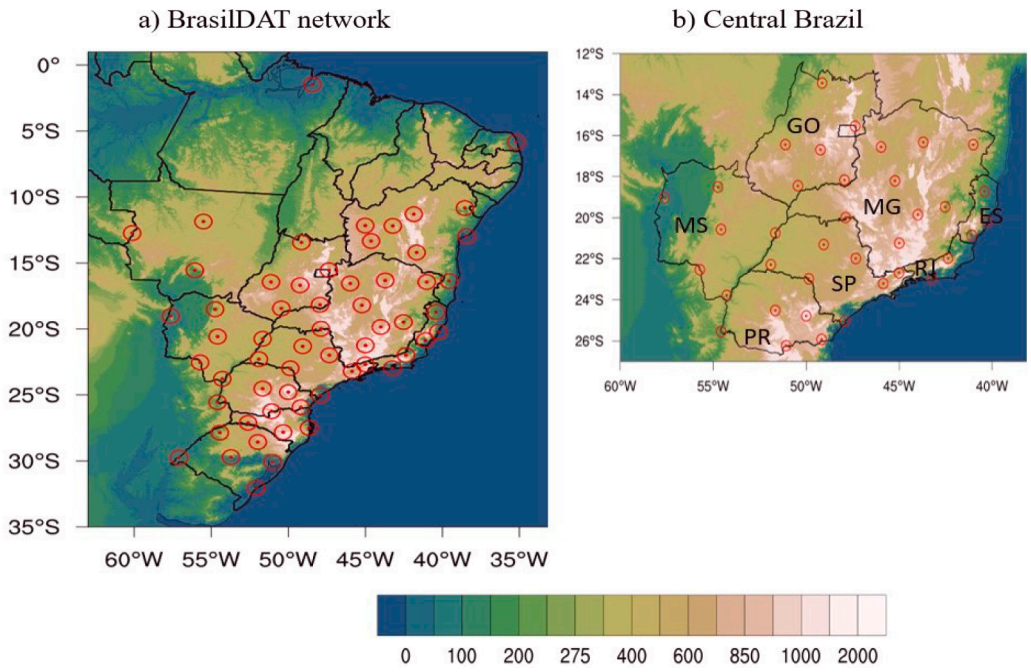

Fig. 1. a) Sensor configuration of the BrasilDAT total lightning detection system with 59 installed sensors, and b) study region in Central Brazil with 37 sensors and the main topographic features (in meters). The region of study includes the States of Mato Grosso do Sul (MS), Goiás (GO), Minas Gerais (MG), Espírito Santo (ES), Rio de Janeiro (RJ), São Paulo (SP) and Paraná (PR).

severity, prevention, detection, mitigation, ignition agents, geographic factors, fire spread, regional characteristics and several other aspects related to human activity (Catry et al., 2009; Martínez et al., 2009; Ojerio et al., 2011; Aldersley et al., 2011; Elia et al., 2019). However, the probability of ignition is not always directly attributed to humans.

The occurrence of natural wildfires has also been reported in several places around the world associated with lightning (Pineda et al., 2014; Clarke et al., 2019; Nadeem et al., 2019; Moris et al., 2020; Rodríguez-Pérez et al., 2020; Nampak et al., 2021). Lightning-caused fires represent 16% of all wildfires within the Continental United States for the period of 1992–2013 and account for 56% of the total acreage burned (Balch et al., 2017). In North America most recent large forest fires were caused by lightning (Veraverbeke et al., 2017). Lightning is also a major cause of wildfire occurrences in Canada, igniting ~45% of total fires and representing more than 85% of the total area burned (Wotton and Martell 2005; Abdollahi et al., 2019). In fact, for fire-prone forests lightning ignition has a higher impact compared to that caused by humans; this because they occur mainly in forest reserves located in remote areas, making it difficult to manage fire suppression, what leads to a more significant burned area (Wang and Anderson 2010).

The number of fires and the total area burned by lightning varies at regional scales. For instance, in boreal forests of northeast China lightning-caused fires accounted for 45% of the events and 5.6% of total burned area (Liu et al., 2012); in Australia it can reach ~30% and represents about 90% of the area burned (Dowdy and Mills 2009; Egloff 2017). In European countries lightning ignitions are more frequent in boreal zones than in Mediterranean regions (Ganteaume et al., 2013). In South America, there is evidence that lightning is a minor factor, about 0.3%, in the ignition of wildfires in Chile (CONAF, 2015; Úbeda and Sarricolea 2016).

In Brazil, lightning and ensuing fires in the Emas National Park, Goiás State, Brazil, in the Cerrado/Savannah biome, were studied by Ramos-Neto and Pivello (2000), accounting for 89% of the wildfires from 1995-1999; for the same park, França et al., (2004) identified 13 events such natural fires in the rainy season of 2002-2003, and Pereira and França (2005) reported 14 additional natural fires in the next rainy season. And more recently, also for the Emas National Park, Schumacher and Setzer (2021) analyzed lightning data in relation to vegetation fires detected by satellite for 2015-2019, identifying 36 cases. However, for most regions in Brazil there are no studies or records about lightning-caused fires, and the country's lightning network has limitations in spatial and temporal scales posing limitations to investigations about lightning-caused fires.

Previous studies attempted to understand the complex role that lightning plays in wildfire occurrences. A lightning-caused fire is characterized by CG lightning, which consist of one or more separate strokes driving charges to the ground (Burrows et al., 2002). Research has shown that the efficiency of lightning in causing ignition is related to the number of events and to various physical properties such as polarity and the presence of long continuing current (e.g., Wotton and Martell 2005; Chen et al., 2015).

The polarity of a CG flash is defined by the net charge that it brings to ground. Positive CG flashes have their discharges usually followed by a low intensity but long duration current. This current is called continuing current. Long continuing currents (LCC) (lasting more than 40 milliseconds) are responsible for most serious lightning damage associated with thermal effects. It is present in approximately 30% of the negative CG flashes and 75% of the positive flashes (Saraiva et al., 2010; Saba et al., 2006a; Saba et al., 2010; Bitzer 2017). As positive flashes have a higher incidence of long continuing current, they are more effective for ignition that the negative flashes. However, thunderstorms usually produce more negative flashes (around 90%) and therefore negative flashes can produce more wildfires than positive flashes (Schultz et al., 2019; MacNamara et al., 2020).

Lightning-caused fires are also associated with dry thunderstorms events, i.e., when the occurrence of lightning is accompanied by little or no precipitation to suppress or extinguish ignitions and are referred to as "dry lightning" (Nauslar et al., 2008). These dry lightning events have been acknowledged to ensure the ignition of largest wildfires (Dowdy and Mills, 2012). Dry lightning can occur in three cases: when precipitation evaporates before reaching the ground; when a thunderstorm is fast moving and significant rainfall do not accumulate on the ground; or, outside the rain shaft (Rorig and Ferguson 2002; Dowdy and Mills, 2009). These events have a great potential to start fires, with less than 1

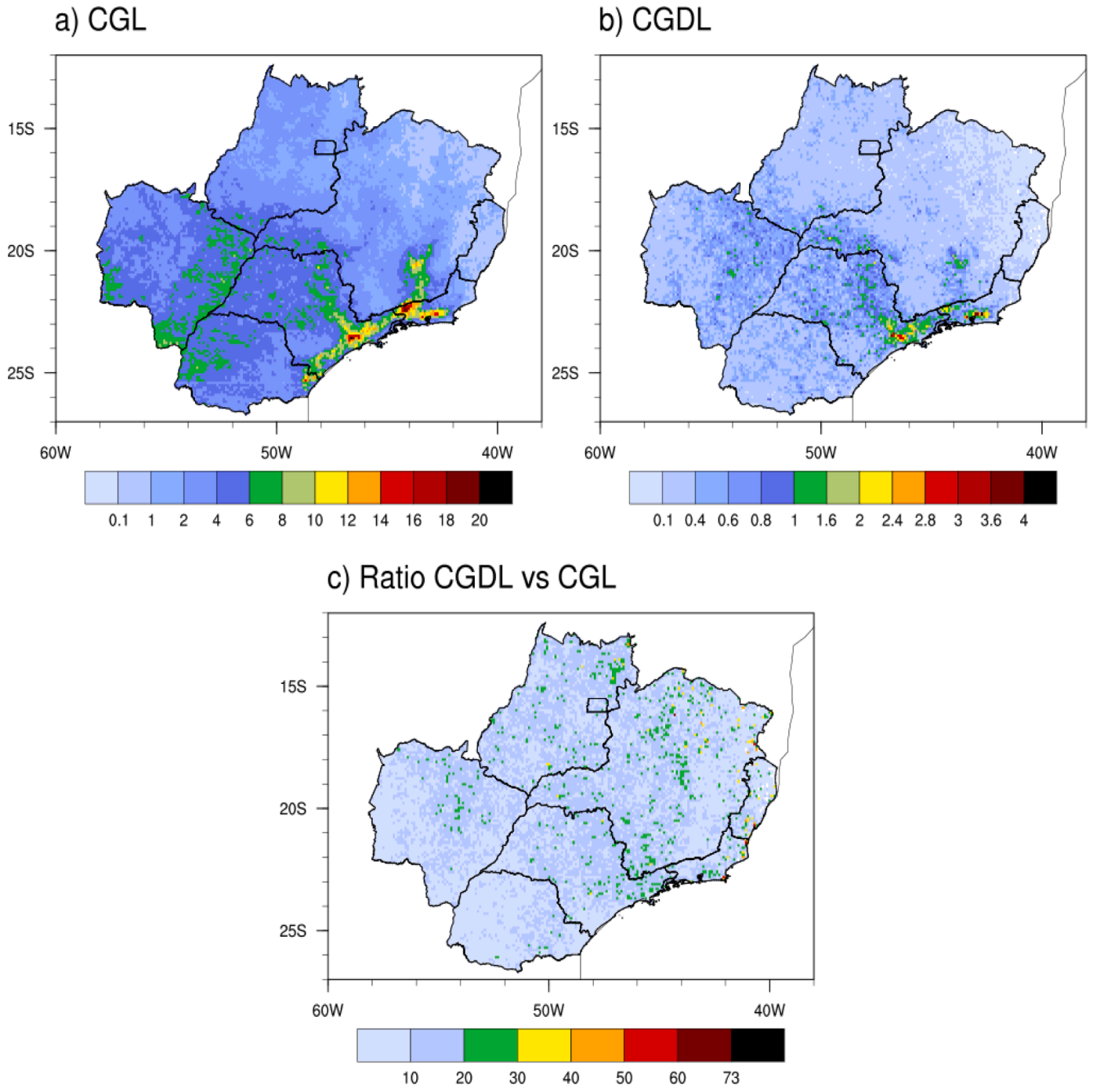

Fig. 2. Spatial distribution of the annual a) cloud-to-ground (CG) lightning and, b) CG dry lightning (CGDL) flash rate density (lightning.km^{-2}.year^{-1}), and c) ratio between CGDL and CG lightning (%) for Central Brazil, from 2015 to 2019, with 10 km spatial resolution.

mm of rainfall, the chance of fire per stroke being about 4 times higher than average (Dowdy and Mills 2012). Although dry lightning events are a good metric to assess ignition potential, in Brazil the precipitation that accompanies lightning in general tends to extinguish fires started by the ignitions (e.g., Ramos-Neto and Pivello, 2000). Dry lightning, however, has not yet been studied in Brazil.

Lightning activity prevails in the tropics and subtropics, and therefore Brazil with its large 8.5*10^{6}km^2 territorial extension, ranks among the regions of highest lightning rates in the world, with about 50 to 100 million CG lightning flashes per year (Albrecht et al., 2016; Christian et al., 2003; Pinto Jr. and Pinto 2018). Fire departments in Brazil report that 99% of vegetation fires are caused by human action, either on purpose or by accident (Macário 2014; Tolentino 2014; G1 2017); a study over conservation areas during for four years concluded that 90% of the wildfires were of anthropic origin (e.g., Santos 2004). Although lightning-caused vegetation fires in Brazil account for a small proportion of the total occurrences, under ongoing climate change the potential for lightning-caused fire is expected to increase (Price 2009; Krause et al., 2014; Singh et al., 2017; Mariani et al., 2018; Li et al., 2020).

Brazil is also a country with intense use of fire by indigenous populations and in agriculture and cattle production and their expansion in previously forested areas; in many cases, fires spread out of control to conservation areas. Every year, with a larger or lesser extent, these fires result in losses of human lives, property, and husbandry, also causing

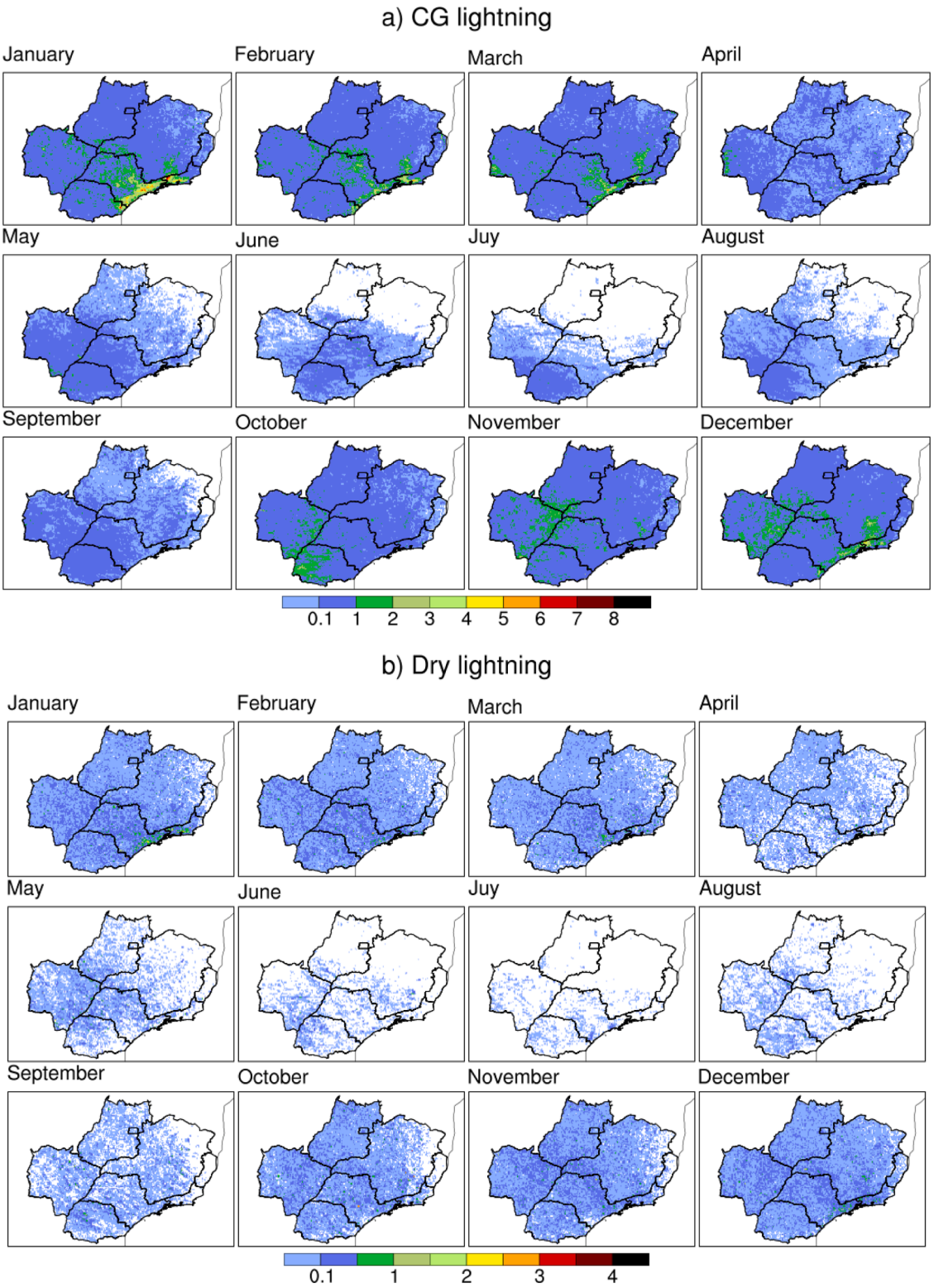

Fig. 3. Spatial distribution of the monthly a) cloud-to-ground (CG) lightning and b) CG dry lightning (CGDL) flash rate density (lightning.km^{-2}.year^{-1}) for Central Brazil from 2015 to 2019, with 10 km spatial resolution.

respiratory diseases in millions of inhabitants and severe damage to natural ecosystems (Campanharo et al., 2019; Fonseca et al., 2019). In 2020, ~26% to 35%, or about 48 × 10^3 km^2 of the "Pantanal" (wetlands) biome were devastated by misuse of fires originating at farms, devastating protected areas, farms, and properties (INPE 2021a; Leal Filho 2021). On average, detections using the MODIS sensor onboard the AQUA satellite amount to 220 thousand fire pixels per year, with a maximum of 470 thousand.year^{-1}; including detections from all available satellites the detections rise to over one million/year (INPE 2021b). Amazingly, despite the relevance of wildfire occurrences almost no information and studies exist about lightning-caused fires in Brazil.

The objective of this study is to quantify occurrences and determine

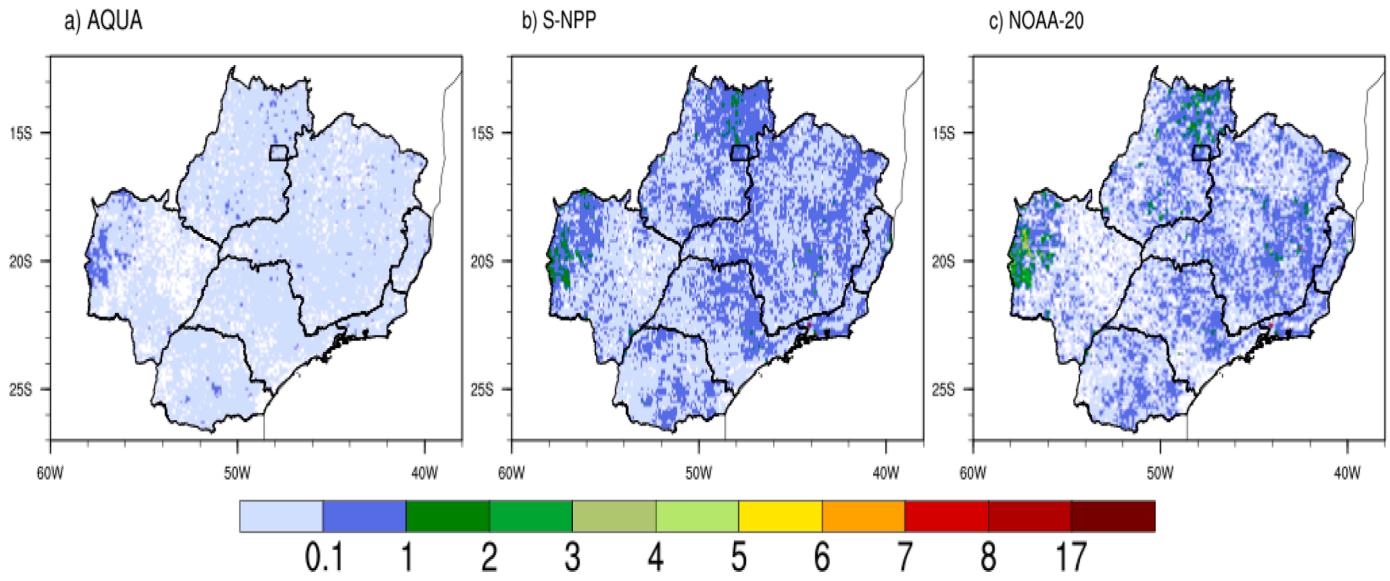

Fig. 4. Spatial distribution of the annual active fires from a) AQUA, b) S-NPP and c) NOAA-20 (fires.km^{-2}.year^{-1}) for Central Brazil from 2015 to 2019, with 10 km spatial resolution. NOAA-20 data only for 2019.

characteristics of lightning related to wildfires ignitions in Central Brazil for the period 2015-2019. We match lightning strokes to vegetation fires detected though satellite remote sensing. Spatial and temporal distributions of CG lightning and CGDL and of active fires also are analyzed, including the connections between them addressing aspects of lightning electricity, wildfire ignition by lightning, and weather conditions. We have produced a first large-scale analysis of lightning-wildfire connection in the country, presenting positive results that can be further expanded to quantify natural wildfires on a regular and automatic way, useful where no regular observations exist. Therefore, our results should help quantify the extent of natural wildfires in contrast to the anthropic use of fire providing scientific knowledge and managerial information in topics ranging from environmental conservation to mitigation of climate-related emissions of gases and aerosols.

The data used and methods applied are detailed in Section 2. Results and discussion are presented in Section 3, including annual and seasonal spatial-time distributions of lightning and fire occurrence, lightning-related wildfires, the relationship between atmospheric conditions, as well as validations of lightning-related wildfires. Conclusions are presented in Section 4.

2. Data and Methods

2.1. Lightning data

CG lightning strokes data from 2015 to 2019 were provided by the Brazilian Lightning Detection Network – BrasilDAT with sensors manufactured by Earth Networks (Naccarato et al., 2012). In the last decade, several improvements were made in the lightning location algorithms reaching a stable configuration in 2014 that resulted in a better-quality control regarding the discrimination between intra-cloud and CG lightning, for more information about the improvements in the lightning location algorithms, refer to Zhu et al., (2016, 2017); as a consequence, nowadays there is no need to remove strokes of less than 15 kA anymore, what encompasses the 2015-2019 period of this study.

Fig. 1a shows the current distribution of the BrasilDAT sensors and detailed description about the network and its lightning sensors techniques are given by Naccarato et al., (2012) and Pinto Jr. and Pinto (2018). The BrasilDAT presents average precision location of 500 m and detection efficiency of 90% for return strokes within the network (Zhu et al., 2016, 2017). The region of study includes the states of Mato Grosso do Sul (MS), Goiás (GO), Minas Gerais (MG), Espírito Santo (ES), Rio de Janeiro (RJ), São Paulo (SP) and Paraná (PR), hereafter referred to as Central Brazil (Fig. 1b); it encompasses the states with the better detection efficiency of CG lightning (e.g., Naccarato and Pinto 2009; Zepka et al., 2014). One must bear in mind that efficiency of the sensor network depends on the intensity of the return stroke. A lightning detection network has lower detection efficiency for low peak current return strokes. As negative return strokes followed by long continuing current have lower peak current, the negative return strokes that start wildfires can be less detectable (Saba et al., 2006b; Saba et al., 2010).

2.2. Active fire data

Active fires used in this study were provided by three satellite sensors, namely: (i) Moderate Resolution Imaging Spectroradiometer (MODIS) onboard the Earth Observation System (EOS) AQUA polar orbiting satellite, early-afternoon overpass, collection 6 version processed by the National Aeronautics and Space Administration (NASA), and where active fires are represented by the center of a 1 km pixel at nadir, from 2015 to 2019 (Giglio et al., 2016); (ii) Visible Infrared Imaging Radiometer Suite (VIIRS) of the Suomi National Polar orbiting Partnership (S-NPP) satellite, with spatial resolution of 375 m, from 2015 to 2019 (Schroeder et al., 2014), and; (iii) the newer VIIRS on the NOAA-20 satellite, also with 375 m of spatial resolution, available for 2019 (Schroeder et al., 2014). All overpasses, at day and nighttime, were used and the data were downloaded from the Wildfire Monitoring Program of the Brazilian National Institute for Space Research (INPE), available at http://www.inpe.br/queimadas/. The VIIRS sensor onboard S-NPP and NOAA-20 satellites detects up to ten times more active fires than the MODIS/AQUA satellite due to its higher spatial and radiometric resolution; however, a relation between MODIS and VIIRS fire detections still lacks in the literature.

2.3. Methods

Lightning density is defined as the number of lightning of a specific type occurring over unit area in unit time, expressed as the number of lightning per square kilometer per year (lightning.km^{-2}.year^{-1}). CG Lightning and active fire counts are defined in this work as the number of lightning strokes and fires within a particular geographical region at the spatial resolution of 1 km^2, except in the spatial analysis where the

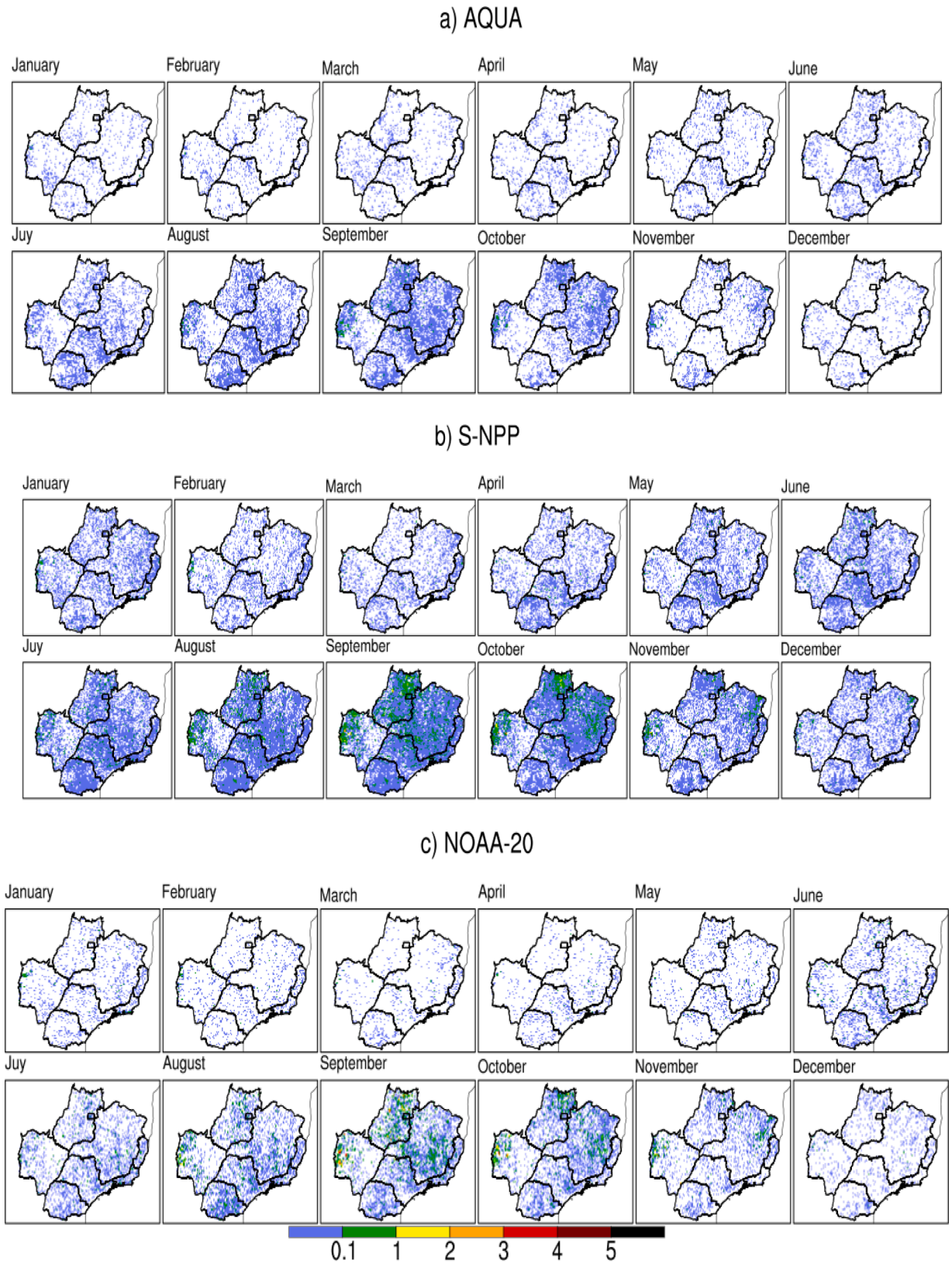

Fig. 5. Spatial distribution of the monthly active fires from a) AQUA, b) S-NPP and c) NOAA-20 (fires.km^{-2}.year^{-1}) for Central Brazil from 2015 to 2019, with 10 km spatial resolution. NOAA-20 data only for 2019.

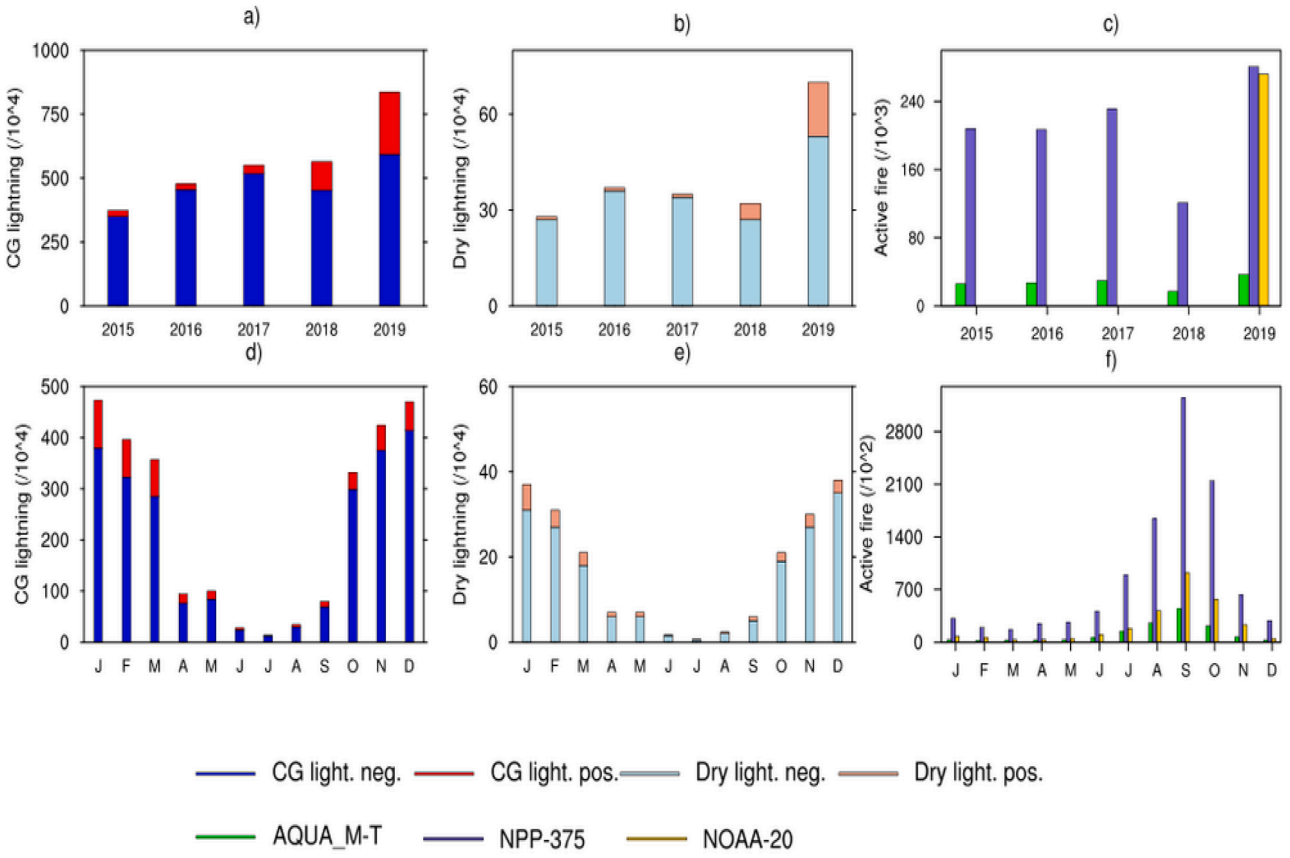

Fig. 6. Annual and monthly frequency of negative and positive cloud-to-ground (CG) lightning, CG dry lightning (CGDL), and active fires for Central Brazil from 2015 to 2019, at 1 km spatial resolution. NOAA-20 fires refer only to 2019.

10 km spatial resolution is used for better representation.

To classify CGDL events, we used daily precipitation data from the Global Precipitation Measurement (GPM) Integrated Multi-satellite Retrievals for GPM (IMERG), available at https://pmm.nasa.gov/data-access/downloads/gpm. The IMERG dataset used in this study was the IMERG Final Run Version 6 (IMERGF-V6) at 0.1° × 0.1° spatial resolution; this product integrates data from satellite radars with records from ground weather stations (Huffman et al., 2019). IMERG was chosen given the fact that Brazil's rain gauge network has a density of one gauge/720 km^2, below the World Meteorological Organization indication of one gauge/575 km^2 (WMO, 1994).

Several studies have evaluated IMERG performance in Brazil and in different parts of the world, providing significant analysis results of IMERG products, for example, in China (Zhou et al., 2021), Nepal (Nepal et al., 2021), Canada (Moazami et al., 2021), Chile (Rojas et al., 2021), and Peru (Llauca et al., 2021). Some studies have also been carried out in Brazil, showing that the IMERG estimates effectively captures the overall spatial patterns of rainfall across the country and can be a satisfactory source of rainfall data to complement the ground precipitation measurements in areas where rain gauges are sparse (Rozante et al., 2018; Gadelha et al., 2019).

Gadelha et al., (2019), comparing precipitation measurements for about 5,000 stations and IMERG data, obtained determination coefficients (R^2) of 0.9, mean error (ME) of 0.08 mm/day, and root mean square error (RMSE) of 0.7 mm/day for the country, and R^2 of 0.9, ME of 0.2 mm/day and RSME of 2.9 mm/day for a region including that of the current study. Siqueira et al., (2021) showed that IMERG product was capable of properly capturing the diurnal cycle of precipitation over our study area. Moreover, IMERG is used with good accuracy in the Fire Risk product of the Wildfire Monitoring Program of the National Institute for Space Research in Brazil (www.inpe.br/queimadas/portal/risco-de-fogo-meteorologia).

There is no established precipitation threshold to define CGDL events, which can vary according to fuel type and weather conditions (Dowdy and Mills, 2012; Vant-Hull et al., 2018). In this study, we used the threshold of less than 2.5 mm.day^{-1} to define CGDL events, consistent with several other studies (e.g., Nauslar et al., 2008; Abatzoglou et al., 2016; Read et al., 2018; Dowdy 2020). CGDL is defined as the number of CG lightning strokes in 1 km^2 grid cells with precipitation below the defined threshold. To match the lightning grid of 1 km^2, the IMERG 10 km base was resampled into 1 km by bilinear interpolation.

Given the lack of field records for wildfires in Brazil as well as for their ignition causes, this study investigates the occurrence of lightning-caused fires by matching satellite-detected active fires with that of lightning. In order to identify the probable lightning candidates (i.e., igniting stroke) for a wildfire we selected all the lightning strokes closest in time and space prior to the fire detection. We defined a buffer area centered at each active fire detected with maximum buffer distance of 1 km (buffer radius of 500 m) and maximum time delay of 48 h between the lightning and fire detections; this because the satellite fire data does not represent the start of the fire, only its detection by a satellite. This approach is in line with other studies (e.g., Dowdy and Mills, 2012; Schultz et al., 2019). The cases of lightning-caused wildfires were classified in two categories: CG lightning matched to fires (CGLF) and CGDL matched to fires (CGDLF).

The new global atmospheric reanalysis ERA5 is used to examine the atmospheric conditions associated with lightning-caused fires. ERA5 is the fifth-generation database produced by the European Centre for Medium-Range Weather Forecasts (ECMWF), available at https://www.ecmwf.int/en/forecasts/datasets/reanalysis-datasets/era5. ERA5 was produced using a sequential 4D-VAR data assimilation scheme with improvement in horizontal resolution to ~30 km (Hennermann and

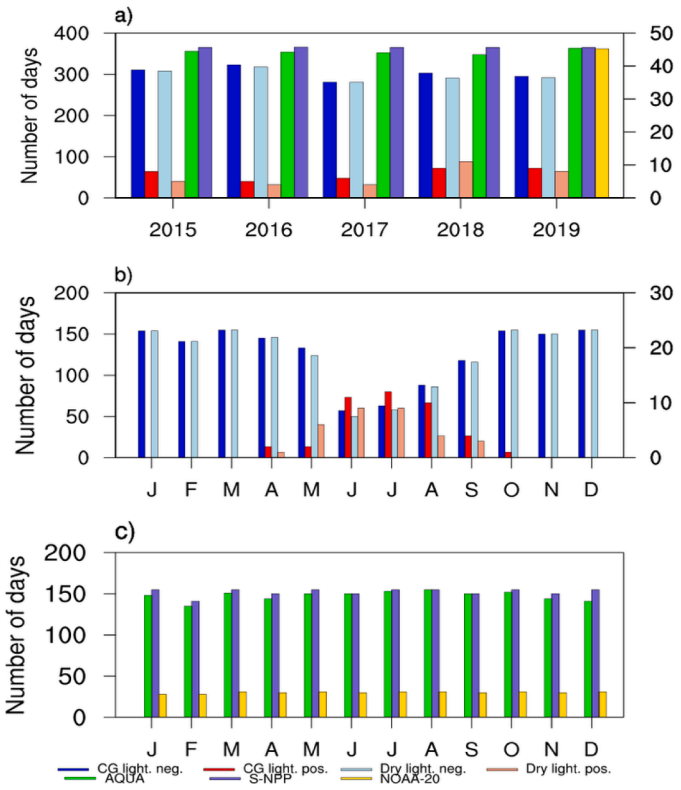

Fig. 7. a) Annual and b-c) monthly distribution of number of days with cloud-to-ground (CG) lightning, CG dry lightning (CGDL) and active fires for Central Brazil, from 2015 to 2019, at 1 km spatial resolution. Y-axes at the right show days only for positive lightning. Cases of several flashes or fires occurring on the same pixel in a single day were considered as one event.

Berrisford 2017). For evaluation against the cases of lightning-caused fires, ERA5 is bilinearly interpolated to 1 km spatial resolution. In this work, we analyzed the 1-hourly meteorological data for the location and time of each lightning candidate to investigate the conditions at the moment of ignition. The selected variables were air temperature, relative humidity, and wind vector components; 1-hourly accumulated precipitation was also analyzed using IMERG product.

3. Results and discussion

3.1. Annual and seasonal spatial distribution

Fig. 2 shows the mean spatial distribution of the annual CG and CGDL density in Central Brazil for a resolution of 10 km x 10 km. It can be seen that stronger lightning activities occur in large urban areas of SP and RJ states, with the maximum CG lightning density of 20 lightning.km^{-2}.year^{-1} in the metropolitan region of SP. Maximum CGDL density is approximately 4 lightning.km^{-2}.year^{-1} in west RJ. This hotspot zone, indicated in yellow and orange in Fig. 2, also presents a steep gradient that extends into SP and MG States coinciding with the local topography of the Serra da Mantiqueira Mountain chain where elevations reach up to 2,800 m. This spatial pattern of events closer to metropolitan regions agrees with other studies which associated lightning in Central Brazil with aerosol emissions and heat island effects (Naccarato et al. 2003; Bourscheidt et al., 2016, Kar and Liou 2019). The ratio between CGDL and CG lightning is also shown in Fig. 2c, providing an indication of the chance of dry lightning. High pixels ratio occurs in parts of the same region with higher CGDL density (Fig. 2b), extending to the state of ES and north of MG, and GO states. These regions are generally drier and have a well-defined season with rainy summers and dry winters.

The monthly distribution shows that lightning seasonality is well-marked, peaking during the wet season between October and March and falling during the dry season between April and September (Fig. 3). Maximum CG and CGDL density occur in January and their minimum in July, with almost no lightning activity during the dry season in states of GO, MG and ES. During the wet season, CG lightning density varies with the region, with highest values recorded in southeast SP and RJ between December and March, whereas for PR and MS between October and December. These distributions can be linked to local weather systems, with thermodynamic and topographical effects having major impacts on the development of lightning storms (e.g., Williams et al., 2005). Previous studies also have indicated the role of orography in the convective process and lightning activity in northeastern and southern Brazil (Bourscheidt et al., 2009, Abreu et al., 2020).

The spatial distribution of active fires for Central Brazil is shown in Fig. 4. The region with higher distribution of active fires is noted in west MS, comprising parts of the Brazilian biomes Pantanal and Cerrado. This incidence is observed by the three satellites, with emphasis on the year 2019 by NOAA-20. Another region with high incidence of active fires is in the state of GO, Cerrado biome, shown by both S-NPP and NOAA-20. The use of fire in agricultural practices is common in these regions and has been the subject of fire control and management policies (Pivello 2011, Alves and Modesto Junior 2020). Also noticed are high values of active fires (up to 17 fire.km^{-2}.year^{-1}) in the same region with a high incidence of lightning in the western region of RJ (see Figures 2 and 4).

Fig. 5 shows the monthly spatial distribution of active fires by three satellites, where the months with highest occurrences are observed during the dry season, between July and October, with a highlight in September. As expected, during the dry season there is an association of weather factors that facilitate the ignition and spread of fire when drought conditions increase litter production as fuel (Collins et al., 2019). It is also worth mentioning that although the peaks of occurrences for fire and lightning occur in different months, CG lightning activity during September and October is remarkably high.

A fire regime can also be related to fire intensity through variables such as the combustion temperature and efficiency, flame height, fuel load, among others (Laris et al., 2020). However, no such information exists for the fire events analyzed, and the use of Fire Radiative Power, FRP, obtained from the fire pixels detected by the satellites is of limited value because it measures only twice a day the temperature at the specific imaging instant, and up to a saturation limit of ~367K.Fire occurrence and fire intensity may have distinct distributions and impacts at global and local scales. For instance, Giglio et al., (2006) investigated the global distribution of fire intensity, showing that in the tropics and subtropics low-fire intensity is associated with forested areas, while higher fire intensity prevails in areas of grassland burning. Conversely, in boreal forests, high fire intensity occurs in areas with large trees and continuous coverage. High fire intensity was also noted across the lower Himalayan hilly region, mostly covered by dense forest (Sannigrahi et al., 2020). Luo et al., (2017), using satellite data, have suggested that fire occurrence and intensity are correlated, where fire occurrence changes with fire intensity following a non-monotonous “humped” relationship, varying with vegetation type, climatic, and anthropogenic conditions.

Kganyago and Shikwambana (2020) analyzed MODIS evaluations of FRP and burned area in Brazil, USA and Australia, considering various vegetation compositions, prevailing meteorological and environmental conditions and anthropogenic activities; significant fire intensity was recorded over forest cover and shrublands, although in the case of Brazil one must consider that the forests burned refer mainly to previously felled trees in the process of deforestation. Additionally, the combination between deforestation and fragmentation of the critical forest edge areas affects the fire occurrence and fire intensity, increasing biomass-burning emissions (Armenteras et al., 2013; Silva Junior et al., 2018; Fischer et al., 2021).

A recent study analyzed fire components in the ecoregions of the Cerrado, the second largest biome in Brazil, showing large spatial

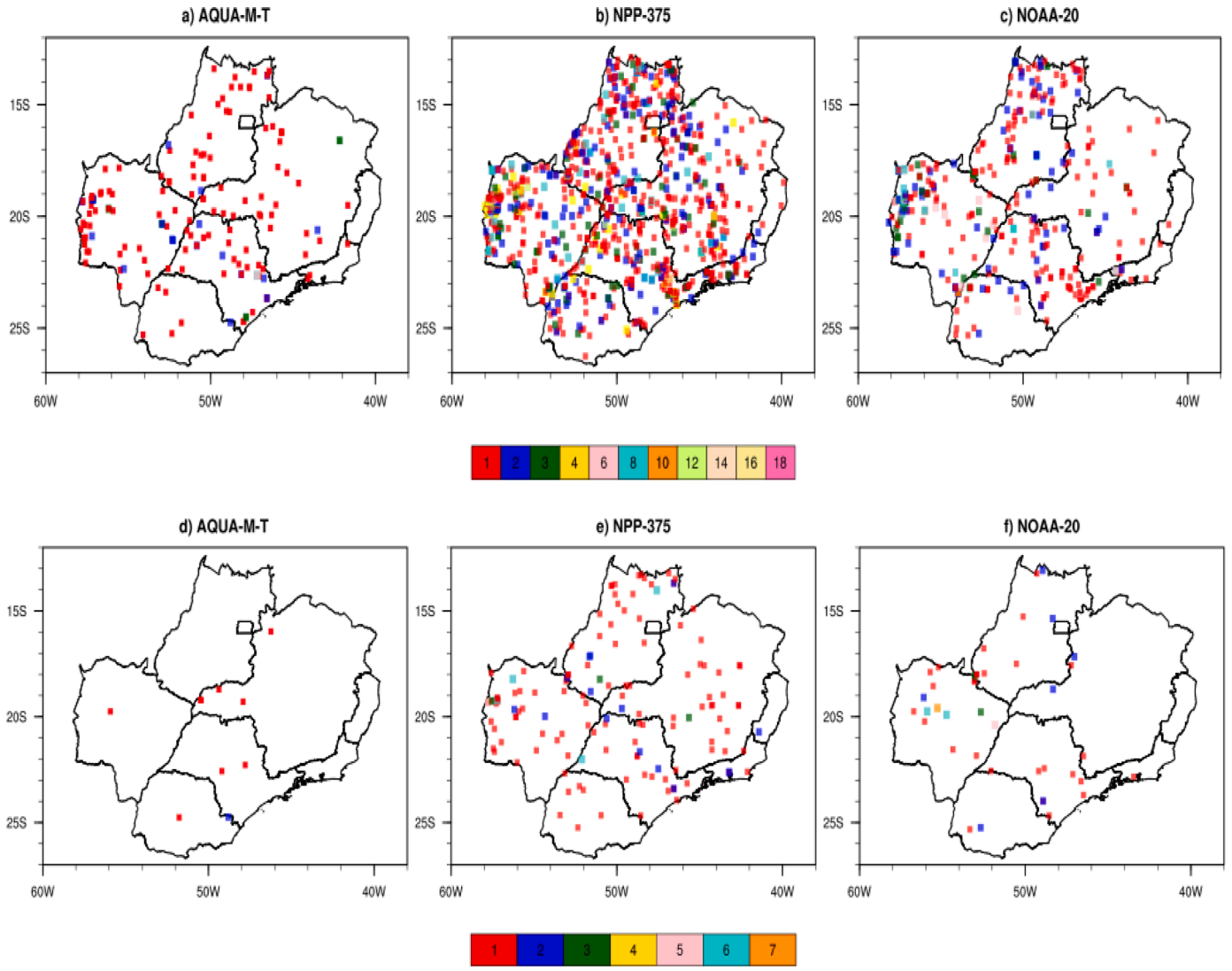

Fig. 8. Spatial distribution of cases a-c) CG lightning matched to fires (CGLF) and d-f) CGDL matched to fires (CGDLF) for Central Brazil, detected with satellites: AQUA and S-NPP from 2015 to 2019 and NOAA-20 for 2019, with 1 km spatial resolution. Label bar values indicate the number of candidates strokes per km^2.

heterogeneity in fire intensity, with high values identified in the limits with the Caatinga and the Amazon biomes. Most ecoregions showed marked seasonality in fire intensity with higher values in the late dry season (Silva et al., 2021), similarly to what was observed in Australia (Oliveira et al., 2015).

3.2. *Frequency and time distribution*

Fig. 6 shows the inter and intra-annual distribution of negative and positive CG and CGDL and active fires for Central Brazil, from 2015 to 2019. On average, 5.6 (0.4) million per year of CG lightning (CGDL) occur in Central Brazil during this period. Characteristics of CG and CGDL in terms of polarity show that negative CG lightning predominate and account for 85% of the total CG lightning and for 88% of the total CGDL. CGDL represents about 7% of the total CG lightning. In general, Central Brazil presents an increase of CG lightning, mainly positive lightning, between 2018 and 2019. This increase is also noted for positive CGDL. Besides that, a significant increase in CG and CGDL activity occurs in 2019 compared to previous years (Fig. 6a,b).

This positive lightning increase with higher occurrences in 2019 is observed in almost all States, except for ES (Figure S1). In fact, in 2019 Central Brazil experienced a widespread positive anomaly of mean surface air temperature of up to 2°C, except for ES, where a negative anomaly of 2°C in relation to the climatology was observed across the ES State (INMET 2020). As previously mentioned, higher temperatures should contribute to lightning activity (e.g., Reeve and Toumi 1999; Romps et al., 2014). Moreover, higher lightning occurrences are observed in MS, SP and MG, with an average of 1.5 (0.1), 1.2 (0.1), 1 (0.09) million.year^{-1} of CG lightning (CGDL), respectively. PR, GO and RJ presented moderate values, with an average of 0.76 (0.04), 0.74 (0.06) and 0.19 (0.01) million.year^{-1} of CG lightning (CGDL), respectively. A lower occurrence was noticed in ES, with 34 (3.6) thousand. year^{-1} of CG lightning (CGDL).

Comparing monthly distributions (Fig. 6d,e), negative and positive CG lightning, as well as CGDL, occur more frequently in the warm and wet months, similarly to the spatial distribution shown in Fig. 3. In general, both CG lightning and CGDL follow an analogous distribution across the year, with an increase of cases starting in October, maximum peak in December and January, and decreasing thereafter. However, the distribution of CG lightning in ES state presents a maximum peak in March and December, while PR shows a peak in October (Figure S2).

For Central Brazil, about 74% of negative CG lightning occurs during the warm season (October and March) against 11% during the cold season (April and September). On the other hand, positive CG lightning corresponds to 13% and 2%, respectively. Negative CGDL accounts to 79% during the warm season and 9.5% in the cold season, whereas

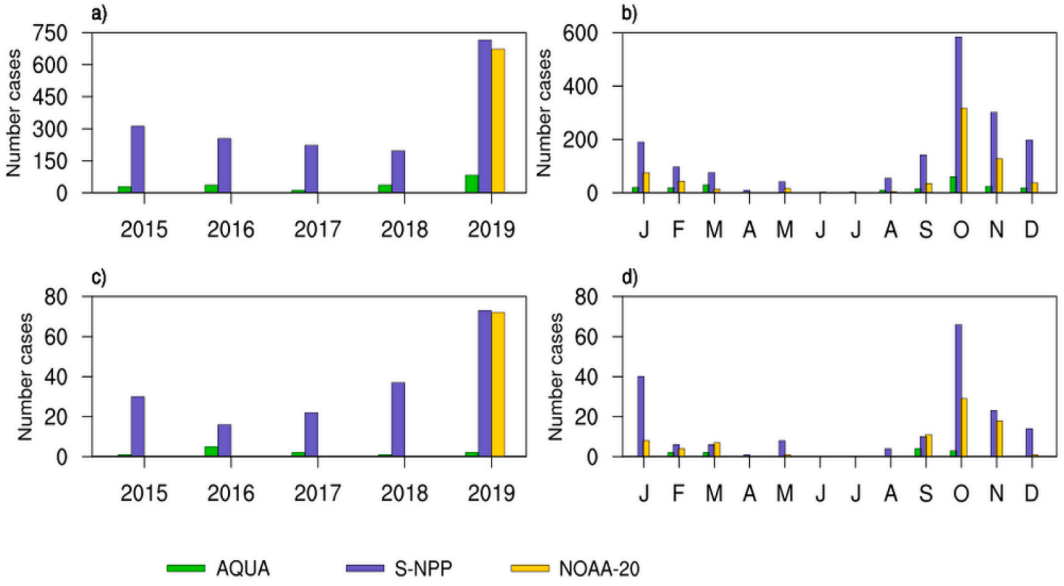

Fig. 9. Annual and monthly distribution of number of cases of a-b) CG lightning matched to fires (CGLF) and c-d) CGDL matched to fires (CGDLF) for Central Brazil, detected with satellites: AQUA and S-NPP from 2015 to 2019 and NOAA-20 for 2019.

positive CGDL only to 9.5% and 2%, respectively.

Active fires in Central Brazil on average reach 27 thousand per year detected by AQUA and 209 thousand per year by S-NPP. For the full dataset, higher values are observed in MG, MS, and GO states, with averages of 8 (59), 6 (42), and 5 (53) thousand/year active fires from AQUA (S-NPP), respectively. A decrease in fire occurrences in 2018 and a significant increase in 2019 in Central Brazil and in almost all states is noticed, mainly in MS (Fig. 6 and S1). This tendency reflects to a large extent that for Central Brazil 2018 was a relatively wet year compared to 2019 (INMET, 2020).

Fig. 6 shows the monthly distribution of active fires for Central Brazil, where 78% and 76% occur between July and October as detected from AQUA and S-NPP, respectively. Agriculture and pastures prevail in the study area and fires, started either on purpose or accidentally, are very frequent. However, they occur mainly at the peak of the dry season (Fig. 6), when rains (and lightning) are rare - up to two or three consecutive months with no rain at all are common from June-September (INPE, 2021b). Therefore, the analysis of lightning intrinsically excludes the agricultural fires. Almost all states have a similar monthly distribution pattern, except ES. Although ES shows a low number of fires, the occurrence is well distributed over the months, with peaks in January and September. RJ state also presents slightly higher numbers during the other months, although with its peak between July and October (Figure S2). This pattern of a temporal distribution of vegetation fires with a marked peak at the dry season resulting mainly from anthropic activities is found worldwide, and has been documented, among others by Giglio et al (2006) and Pausas and Keeley 2021; consequently, lightning has virtually no relation to such fires, except in the cases of pyrocumulonimbus lightning that so far have not yet been observed in the study area.

Fig. 7 shows the annual and monthly distributions of number of days for negative and positive CG and CGDL, and of active fires for Central Brazil between 2015 and 2019. In general, the annual variability is small and there is no marked change in the occurrence of negative lightning or fires. The occurrence of negative CG (CGDL) ranged from 281 to 311 (281 to 308) days, while positive CG (CGDL) ranged from 5 to 9 (4 to 11) days. For days with active fires, AQUA data ranged between 348 to 363 days and S-NPP detected fires in all days.

The monthly distribution of the number of days for negative and positive lightning is inversely proportional for Central Brazil, that is, there is a greater occurrence of negative lightning days in the warm season, while positive lightning days occur in the cold season (Fig. 7b). This effect is clearly seen in the states of SP and PR (not showed) and may be associated with the nature of the convection during the cold season, for example, the frequency and intensity of frontal systems that reach these states providing more lightning storms than RJ and ES States. In addition, the increase in positive lightning occurrence during the cold season may be associated with the presence of smoke aerosols, in line with the suggestion of Fernandes et al., (2006).

For the cumulative period of 2015-2019, positive lightning occurs in less than 15 days per month compared to over 100 days of negative lightning. The distribution of number of days with active fires is relatively stable and does not show the same variability as the monthly distribution of active fire counts (see Figures 7c and 6f). This shows that although a lower number of active fires is found between November and June, even so, the number of days with fires is relatively high in all months, totaling in the five years of 2015-2019 between 40 to 135 days for AQUA and 90 to 150 days for S-NPP.

3.3. *The relationship between lightning and fire occurrence*

To further illustrate the occurrence of lightning-caused fires in Central Brazil, Fig. 8 shows the spatial distribution of the selected fire lightning candidates, CGLF and CGDLF. As expected, the number of cases of CGLF is greater than CGDLF, and S-NPP and NOAA-20 present more fire pixels in relation to AQUA. It is noted that fluctuations in the incidence of fires among sensors result from differences in the time interval coverage, as well as due to their distinct horizontal resolution. Nevertheless, the three satellites indicate candidates for lightning-caused fires throughout Central Brazil. This result is relevant because lightning has been recognized as an ignition source restricted to the Brazilian Cerrado (e.g., Pivello 2011). Indeed, the peak density of cases is noted in the states of MS and GO (Cerrado biome), with a maximum of 18 lightning.km^{-2} in respect to CGLF and 7 lightning.km^{-2} for CGDLF.

Of relevance is also the large number of lightning-related wildfire cases in 2019 detected by NOAA-20, indicating that most lightning candidates during 2015-2019 occurred in 2019. As previously showed, there is no clear connection in the increase in fires and the occurrence of lightning, except in 2019 (see Fig. 6), which presents a higher frequency of active fires and lightning activities. This shows that although the highest number of fires is caused by humans, the increase of lightning activity contributes to the increase of natural fires, as detected by the

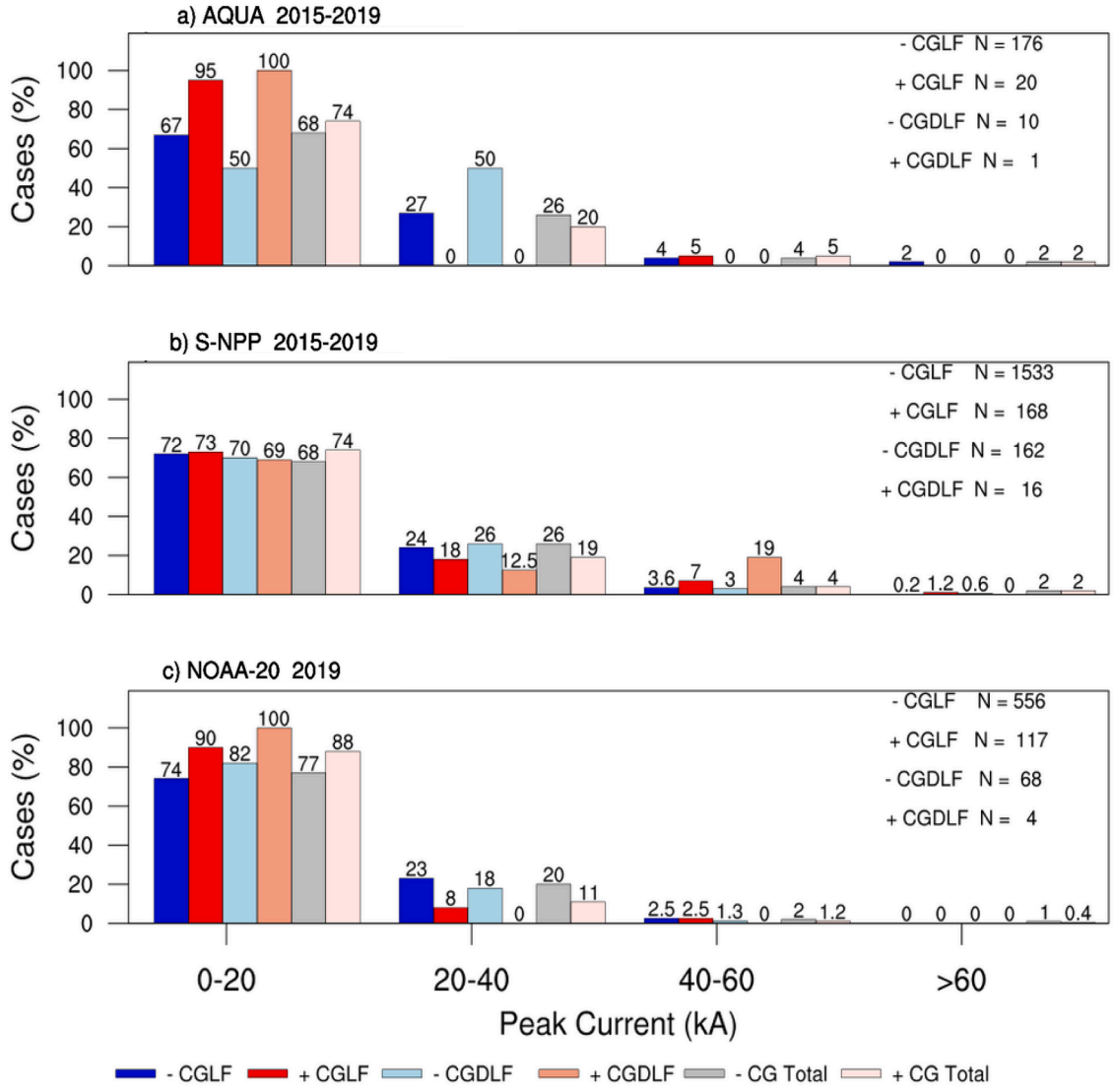

Fig. 10. Percentage of negative/positive CG lightning matched to fires (CGLF), CGDL matched to fires (CGDLF) and CG total lightning (i.e., not associated with a fire) in relation to peak current.

significant number of cases of CGLF and CGDLF in 2019 compared to other years.

Concerning the number of lightning candidates estimated by the three satellites, CGLF presents a total of 196 candidates with AQUA and 1701 with S-NPP, for the same period. Considering only 2019, 673 candidates with NOAA-20. For CGDLF, 11 with AQUA, 178 for S-NPP, and 72 for NOAA-20. The proportion of lightning candidates to total active fires in Central Brazil between 2015 to 2019 is less than 0.15%. However, it may happen that the number of active fires is related to fires that persisted for more than one day, sensitizing several pixels in consecutive days and producing a lower rate between selected candidates and active fires.

Fig. 9 shows the annual and monthly distribution of CGLF and CGDLF candidates where a large number of cases are concentrated in the year 2019; this year alone accounted for about 42% of CGLF and 18 % of CGDLF in relation to total cases detected by AQUA, and 42 % of CGLF and 41 % of CGDLF for S-NPP.

Additionally, there is no evidence of an increase in the occurrences of CGLF candidates between 2015 and 2019; on the contrary, CGDLF shows an increase in cases between 2016 to 2019 by S-NPP. Concerning a seasonal distribution, most lightning candidates occur in October, the second month with the highest occurrence of active fire, corresponding to the transition period from dry to rainy season (see Figures 6f and 9b, d). The distribution of lightning candidates in relation to polarity and peak current with respect to CGLF and CGDLF cases from three satellites is shown in Fig. 10. Negative CGLF and CGDLF candidates accounts for 91% of the total lightning candidates from AQUA and S-NPP. In general, most cases of CGLF and CGDLF present negative as well as positive lightning intensity in the range of 0-20 kA, with percentages between 50 % and 100 %.

This range is associated with low current intensity; however, it presents great potential for damage and risk of forest fires due to the high frequency of lightning in this range and presence of LCC. There is a consensus that lightnings with LCC have a greater potential to ignite a fire, and not polarity itself (Fuquay et al., 1967; Rakov and Uman, 2003; Larjavaara et al., 2005). For Brazil, Saba et al., (2010), based on high-speed video records showed that negative strokes followed by LCC occur with peak currents below 20 kA while positive strokes followed by LCC may present any value of peak current. It is also interesting to note that the proportion of positive candidates is higher above 40 kA for S-NPP cases. This agrees with the fact that positive flashes usually have higher peak current return strokes (Saba et al., 2010). Further, the selected candidates do not present distinct electrical characteristics from the total CG lightning strokes that are not associate with fires (Fig. 10).

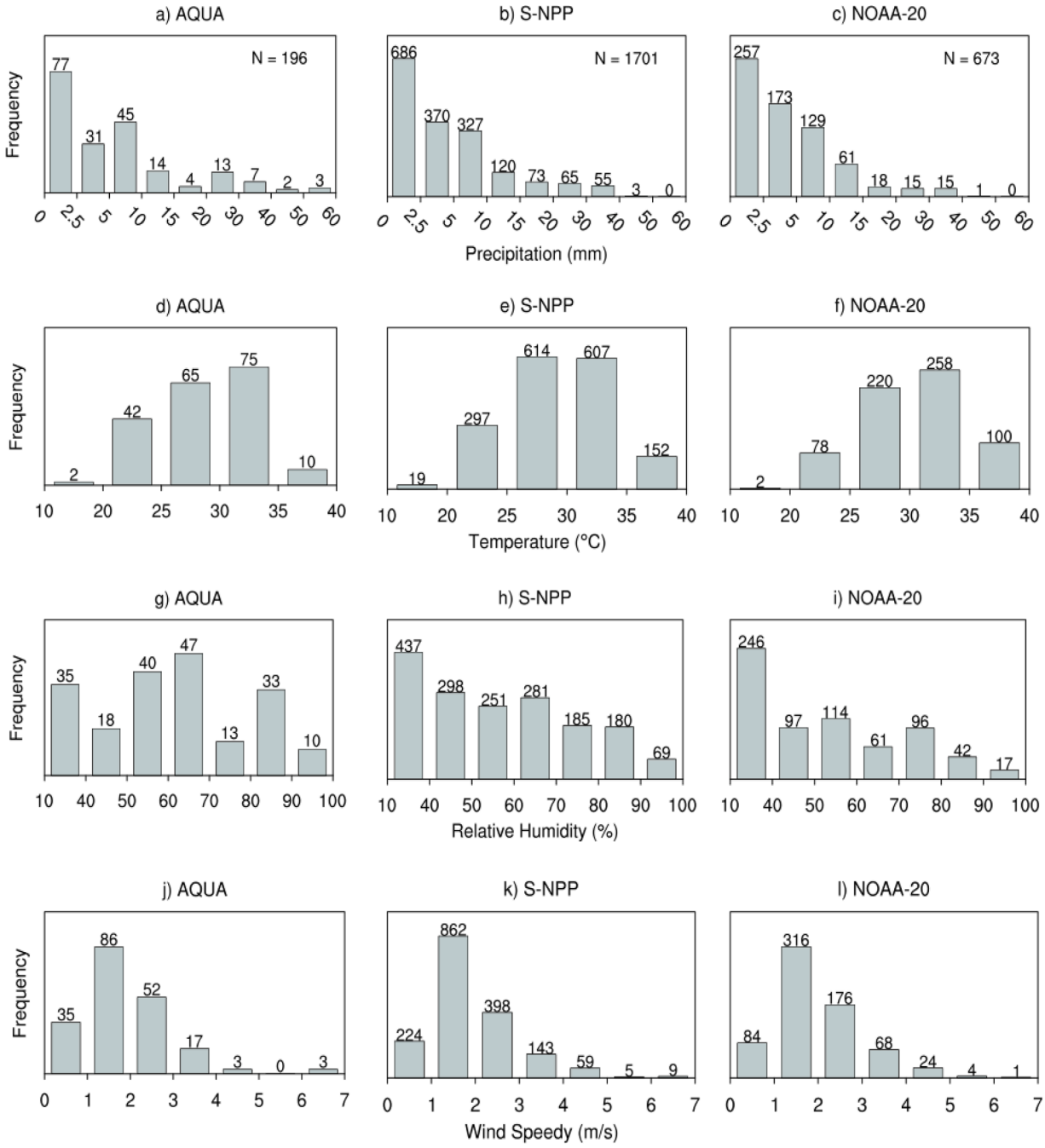

Fig. 11. Frequency distribution of CG lightning matched to fires (CGLF) in relation to: a-c) the hourly accumulated precipitation (mm), d-e) air temperature at 2 m (°C), f-h) relative humidity (%) and wind speedy (ms^{-1}).

In general, these results indicate that the main characteristics of lightning-caused fires in Central Brazil are driven by negative return strokes with low (< 20 kA) peak current, contrary to accepted theories in which positive strokes are more likely to ignite wildfires (e.g., Wotton and Martell 2005; Moris et al., 2020). However, this result is in line with the recent findings observed by Schultz et al., (2019) and MacNamara et al., (2020). They found that 90% of the wildfires in the United States were started by negative CG lightning. In a similar study for Finland, Larjavaara et al., (2005) showed that positive and negative strokes ignite forest fires with equal probability. Pineda et al., (2014) had reached similar results and found polarity percentages similar to the climatological and moderate peak current over Catalonia, Spain. Further, parameters like the peak current and polarity can be affected by the local characteristics and also by thermal and aerosol effects (e.g., Naccarato et al., 2003; Seity et al., 2001; Wang et al., 2021).

3.4. Atmospheric conditions associated with lightning-related wildfires

To examine atmospheric characteristics at the moment of ignition associated with lightning-related wildfires, Fig. 11 shows the frequency of cases in relation to 1-hourly meteorological data for the location and time of each lightning candidate. For precipitation, higher frequency is associated with the CGDL range, where the total number of candidates with up to 2.5 mm at the moment of ignition corresponds to about 39%, 40% and 38% of the detections by AQUA, S-NPP and NOAA-20, respectively. Although this higher frequency accounts for a little less than half of the total cases, most lightning candidates occur with less than 10 mm of precipitation at the time of ignition, with about 78% of

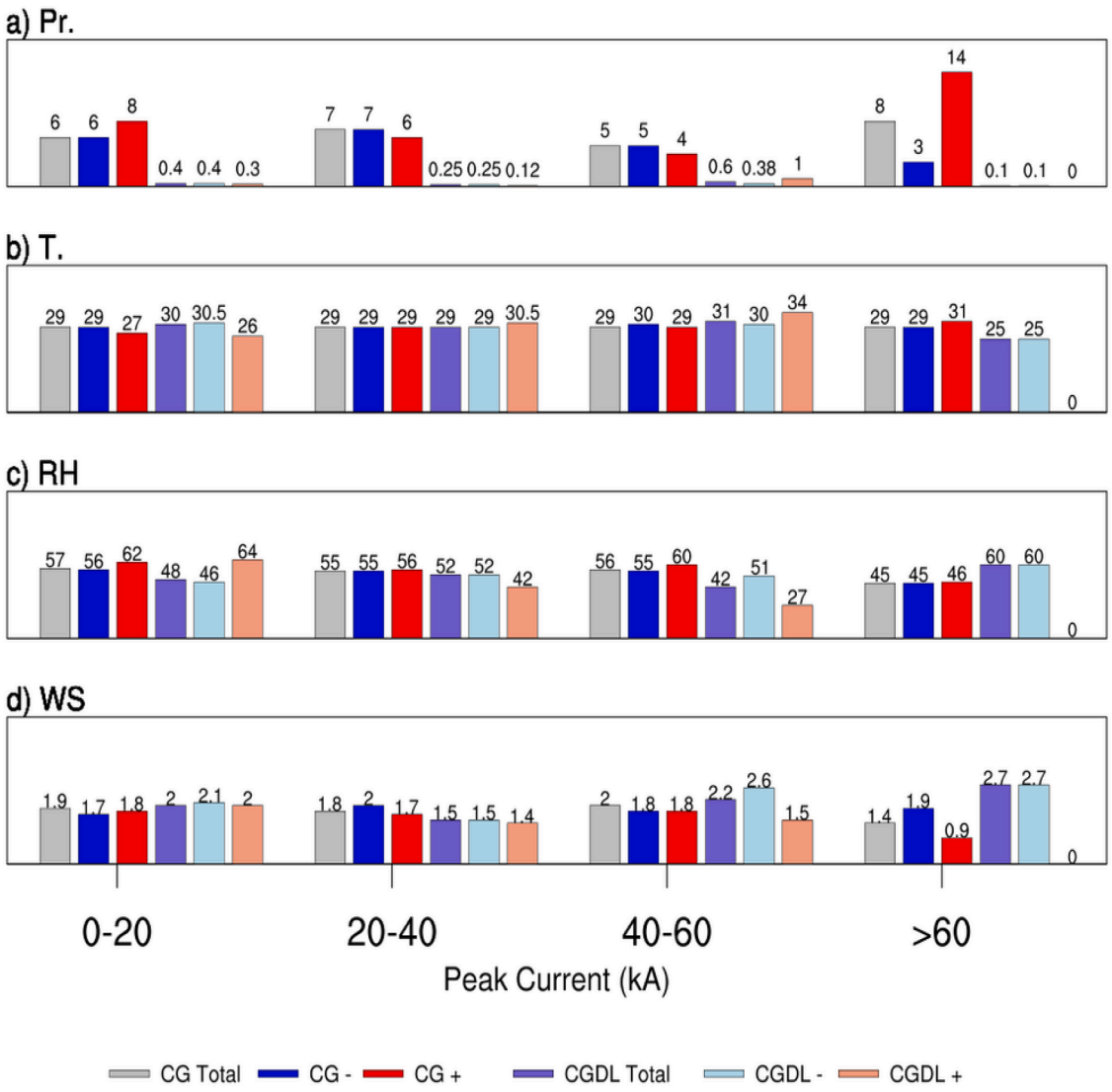

Fig. 12. Local mean atmospheric conditions at the time of lightning candidates occurrence associated with negative (-) and positive (+) CG lightning matched to fires (CGLF), CGDL matched to fires (CGDLF) and CG total lightning according to the range of peak current detected by S-NPP.

the cases detected by AQUA, 81% by S-NPP and 83% by NOAA-20, respectively.

Additionally, most cases are driven by high air temperature in the range 30 to 35°C. For relative humidity, higher frequency is noted below 40%, with a gradual decrease shown by S-NPP and NOAA-20. On the other hand, the relative humidity frequency for AQUA shows higher values in the range between 50-70%. In addition, there is a greater proportion of lightning candidates from S-NPP and NOAA-20 detections associated with high humidity. Concerning wind speed, the atmospheric conditions for most cases showed very low values, between 1 to 2 $m \cdot s^{-1}$.

Further assessment of atmospheric characteristics and lightning-related wildfires is investigated according to the peak current range (Fig. 12). Regarding the mean atmospheric conditions associated with the range between 0-20 kA in which most cases are found, the CGLF (CGDLF) cases are dictated by low precipitation, 6 mm (< 1 mm), high surface temperature between 29 °C (30 °C), moderate relative humidity, 57 % (48 %) and low wind speed of ~ 2 $m.s^{-1}$ for both. CGLF positive candidates show an increase in precipitation and relative humidity compared to negative candidates. These results are in line with the thresholds discussed by Dowdy and Mills (2012), with increased chance of fire per stroke for temperature above 26°C, wind speed less than 5 $km \cdot h^{-1}$, and lower relative humidity, with a higher chance of fire in the range of about 35%–50%. In general, the higher the temperature and the lower the wind speed and relative humidity, the higher the chance of fire per stroke.

A similar atmospheric pattern has been obtained by Shikwambana and Kganyago (2021) with moderate winds of ~5 m/s, temperatures between 32 and 42°C and relative humidity about 30–50% associated with wildfires that occurred in the United States of America, Brazil, and Australia. Sevinc et al., (2020) showed that lightning induced wildfires in Turkey also occurs under high humidity. In fact, relative humidity plays an important role in the formation of thunderstorms. Shi et al., (2018) discussed the role of relative humidity in the storm microphysics development, electrification, and lightning discharges.

3.5. *Validation of lightning-related wildfires*

An effort is made to validate the detected cases of lightning-caused fires inside protected areas using information from the Chico Mendes Institute for Biodiversity Conservation (ICMBio), as summarized in Table 1. The dates of the field reports were compared to the satellite-detected fires and when there were no active fires on the reported day we verified the presence of active fires up to ten days before or after. This is indicated in the Table 1 as a probable detection (PD) to identify

Table 1
Cases of lightning wildfires recorded in Central Brazil between 2015 and 2019 by ICMBio. Total candidates refer to the number of cases identified in each national park between 2015 and 2019, according to the AQUA-S-NPP-NOAA-20 satellites.

Case	Date	Unit Conservation	State	Match *	Total candidates
01	20150320	Parque nacional das Emas	GO	D	01-13-08
02	20150930	Parque nacional das Emas	GO	PD (26)	01-13-08
03	20151019	Parque nacional das Emas	GO	D	01-13-08
04	20151111	Parque nacional da Chapada dos Veadeiros	GO	D	01-13-02
05	20161110	Parque nacional das Emas	GO	D	01-13-08
06	20161208	Parque nacional das Emas	GO	ND	01-13-08
07	20171007	Parque nacional das Emas	GO	D	01-13-08
08	20171023	Parque nacional das Emas	GO	PD* (24)	01-13-08
09	20180926	Parque nacional das Emas	GO	ND	01-13-08
10	20190117	Parque nacional das Emas	GO	D	01-13-08
11	20190203	Parque nacional das Emas	GO	PD * (02)	01-13-08
12	20190205	Parque nacional das Emas	GO	D	01-13-08
13	20190218	Parque nacional Grande Sertão Veredas	MG	ND	-
14	20190226	Parque nacional de Ilha Grande	PR	ND	0-05-02
15	20190409	Parque nacional das Emas	GO	ND	01-13-08
16	20190902	Parque nacional das Emas	GO	D*	01-13-08
17	20191030	Parque nacional das Emas	GO	D*	01-13-08
18	20191111	Parque nacional Serra da Canastra	MG	PD * (03)	01-08-08
19	20191226	Parque nacional das Emas	GO	D	01-13-08
20	20191226	Parque nacional da Chapada dos Veadeiros	GO	D	01-13-02
21	20191227	Parque nacional da Chapada dos Veadeiros	GO	D	01-13-02

* = Match with CGLF or CGDLF cases;
D = detected from three satellites;
ND = not detected from three satellites;
PD = probable detection (day)

possible inconsistencies in the field reports. Also, to illustrate if it was a case of a quickly suppressed fire or of a day with clouds, when fires cannot be detected by the satellites, the event was reported as not detected (ND).

From a total of 21 cases of lightning ignition in the field reports, five are not detected by the three satellites, probably for the reasons already mentioned. Five cases match those detected by CGLF or CGDLF, of which two cases match the reported field dates, and another three cases are probable detections with close dates. About nine cases detected by the three satellites do not match the location and date of the CGLF or CGDLF cases; this may be associated with errors in the field reports, when the cause was logged as natural rather than anthropogenic or unknown. Although many cases of CGLF and CGDLF are detected inside national and state parks and in nearby regions (see total candidates on Table 1), the field reports are partial and there should be more events, even those in other conservation units, that did not report.

4. Concluding remarks

In this study, we investigated occurrences and characteristics of lightning strokes matched to vegetation fires detected by satellites during the 5-year period from 2015 to 2019 over Central Brazil. To our knowledge, no large-scale studies have analyzed lightning candidates for wildfires in Brazil. Thus, this work provides new information in terms of meteorological features, polarity, and peak current of lightning-caused wildfires occurrence. The use of active fires in remote sensing data proved to be a good alternative for investigating lightning-caused fires in the absence of a forest fire database with attribution of ignition sources in the country.

We additionally presented the first known characterization of the spatial and temporal distribution of dry lightning strokes for Central Brazil. Results showed similar features about lightning density, polarity, and peak current in relation to CG lightning events. Geographical distribution of lightning density was evident over the main mountain ranges and large urban areas of SP and RJ States, with the maximum CG lightning density of 20 lightning.km^{-2}.year^{-1} and 4 lightning.km-^{2}.year^{-1} in relation to CGDL. Regarding seasonality, the highest occurrence of lightning was registered during the warm and wet season, between October to March; oppositely, fires occurred mainly in the dry season, between July and October as detected by three satellites, and indicating their predominantly anthropic origin.

The number of CG lightning in Central Brazil from 2015 to 2019 presents on average 5.6 million.year^{-1}, whereas for CGDL about 0.4 million.year^{-1}. Concerning polarity, negative lightning is predominant, accounting about 85% and 88% of the total CG lightning and CGDL, respectively. For Central Brazil, a major number of days of negative lightning was observed in the warm and wet season, while positive lighting occurred in the cold and dry season. Active fires in Central Brazil showed an average frequency of 27 thousand.fires.year^{-1} in the AQUA satellite monitoring and 209 thousand.fires.year^{-1} with S-NPP. For 2019, S-NPP and NOAA-20 detections showed almost no difference.

We searched for the probable wildfire lightning candidates in Central Brazil based on the location of fires detected by three satellites and their distance and time interval to the lightnings. A total of 196 and 170 (11 and 178) cases of lightning matched to fires – CGLF (CGDLF) were estimated with AQUA and S-NPP, respectively, during 2015 to 2019. Considering the year 2019, NOAA-20 presented a total of 673 cases for CGLF and 72 for CGDLF.

These results demonstrate that, although in smaller numbers, there are fire candidates related to the occurrence of CGDL events, contrary to the common hypothesis that dry lightning is not expected in Brazil. Besides, the occurrence of CGDLF candidates showed an increase of between 2016 to 2019.

In general, our results suggest that lightning-caused wildfires tend to occur with low precipitation, moderate relative humidity, high temperature, and low wind speed. On the other hand, CGDLF cases occur with precipitation values below 1 mm and lower relative humidity than CGLF cases. We have found that lightning candidate intensity was mostly less than 20 kA. For this peak amplitude, local mean atmospheric characteristics at the time of occurrence of the CGLF (CGDLF) cases were driven by low precipitation between 6 mm (< 1 mm), moderate relative humidity, 57 % (48 %), and high temperature of $\sim$30 $^{\circ}$ and low wind speed of $\sim$ 2 m.s^{-1}.

Most lightning candidates presented polarity characteristics similar to climatological ones, with a negative predominance. Our results contradict some studies which suggest that positive strokes are more likely to ignite a forest fire than negative ones (e.g., Moris et al., 2020); however, it has been noted that this feature varies according to the study region (Larjavaara et al., 2005; MacNamara et al., 2020). Our results also agreed with the findings of others studies in terms of polarity, peak current and local meteorology features of lightning candidate ignition (e.g., Pineda et al., 2014; Moris et al., 2020).

Some limitations of the method used to identify lightning candidates

should be mentioned, as the impossibility to detect fires with satellites under cloud overcast conditions, when the sensors also tend to miss fires of short duration and small extent and the lightning detection system may not detect low peak current strokes. Errors or lack of records in field reports of natural fire occurrences may also hamper the validation of the results. Considering such limitations, the main results of this study and the number of lightning-caused fires in Central Brazil should present discrepancies compared to studies based on lightning candidates from forest fire records of fire brigades.

Nevertheless, this study advances the knowledge on lightning-caused wildfires in Brazil, contributing to the scientific understanding of fire ignition sources and bringing new perspectives for the development of wildfire hazard models. The use of remote sensing of fires can be a useful tool to analyze the relation between lightning and wildfires in areas with wildfire risk, assisting decision-making and fire management, in particular for protected and conservation areas.

Further analysis beyond the scope of this paper is needed to narrow the precipitation thresholds used to classify CGDL events in Brazil and obtain more consistent local precipitation data. Future work should also test other buffer distances and holdover time to investigate the relationships between the satellite detections of wildfires and lightning in Brazil.

Declaration of Competing Interest

The authors declare that they have no known competing financial interests or personal relationships that could have appeared to influence the work reported in this paper.

Acknowledgements

We are grateful to the MCTIC-World Bank Project FIP-FM Cerrado/ NPE- Risco (P143185/ TF0A1787), Development of Forest Fire Prevention Systems and Monitoring of Vegetation Cover in the Brazilian Cerrado. We thanks to João Paulo Morita, Coordinator of Fire Prevention and Fighting at ICMBio, for the information of occurrences of lightning fires.

Supplementary materials

Supplementary material associated with this article can be found, in the online version, at doi:10.1016/j.agrformet.2021.108723.

References

Abatzoglou, J.T., Kolden, C.A., Balch, J.K., Bradley, B.A., 2016. Controls on interannual variability in lightning-caused fire activity in the western US. Environ. Res. Lett. 11 https://doi.org/10.1088/1748-9326/11/4/045005.

Abdollahi, M., Dewan, A., Hassan, Q.K., 2019. Applicability of remote sensing-based vegetation water content in modeling lightning-caused forest fire occurrences. ISPRS Int. J. Geo-Info. 8 https://doi.org/10.3390/ijgi8030143.

Abreu, L.P.De, Gonçalves, W.A., Mattos, E.V, Albrecht, R.I., 2020. Assessment of the total lightning fl ash rate density (FRD) in northeast Brazil (NEB) based on TRMM orbital data from 1998 to 2013. Int. J. Appl. Earth Obs. Geoinf. 93, 102195 https://doi.org/10.1016/j.jag.2020.102195.

Albrecht, R.I., Goodman, S.J., Buechler, D.E., Blakeslee, R.J., Christian, H.J., 2016. Where are the lightning hotspots on Earth? Bull. Amer. Meteor. Soc. 97, 2051–2068. https://doi.org/10.1175/BAMS-D-14-00193.1.

Aldersley, A., Murray, S.J., Cornell, S.E., 2011. Global and regional analysis of climate and human drivers of wildfire. Sci. Total Environ. 409, 3472–3481. https://doi.org/10.1016/j.scitotenv.2011.05.032.

Alves, R., Modesto Junior, M.D.S., 2020. Roça sem fogo: da tradição das queimadas à agricultura sustentável na Amazônia. Embrapa Amazônia Oriental-Livro técnico (INFOTECA-E).

Armenteras, D., González, T.M., Retana, J., 2013. Forest fragmentation and edge influence on fire occurrence and intensity under different management types in Amazon forests. Biological Conserv. 159, 73–79.

Balch, J.K., Bradley, B.A., Abatzoglou, J.T., Chelsea Nagy, R., Fusco, E.J., Mahood, A.L., 2017. Human-started wildfires expand the fire niche across the United States. Proc. Natl. Acad. Sci. U. S. A. 114, 2946–2951. https://doi.org/10.1073/pnas.1617394114.

Bitzer, P.M., 2017. Global distribution and properties of continuing current in lightning. J. Geophys. Res. Atmos. 122, 1033–1041. https://doi.org/10.1002/2016JD025532.

Bond, W.J., Woodward, F.I., Midgley, G.F., 2005. The global distribution of ecosystems in a world without fire. New Phytol. 165, 525–538.

Bourscheidt, V., Pinto, O., Naccarato, K.P., 2016. The effects of Sao Paulo urban heat island on lightning activity: decadal analysis (1999–2009). J. Geophys. Res. Atmos. 121, 4429–4442. https://doi.org/10.1038/175238c0.

Bourscheidt, V., Pinto, O., Naccarato, K.P., Pinto, I.R.C.A., 2009. The influence of topography on the cloud-to-ground lightning density in South Brazil. Atmos. Res. 91, 508–513. 10.1016/j.atmosres.2008.06.010.

Bowman, D.M.J.S., Balch, J.K., Artaxo, P., Bond, W.J., Carlson, J.M., Cochrane, M.A., D'Antonio, C.M., DeFries, R.S., Doyle, J.C., Harrison, S.P., Johnston, F.H., Keeley, J. E., Krawchuk, M.A., Kull, C.A., Marston, J.B., Moritz, M.A., Prentice, I.C., Roos, C.I., Scott, A.C., Swetnam, T.W., Van Der Werf, G.R., Pyne, S.J., 2009. Fire in the earth system. Science 324, 481–484. 10.1126/science.1163886.

Burrows, W.R., King, P., Lewis, P.J., Kochtubajda, B., Snyder, B., Turcotte, V., 2002. Lightning occurrence patterns over Canada and adjacent United States from lightning detection network observations. Atmos. - Ocean 40, 59–80. https://doi.org/10.3137/ao.400104.

Campanharo, W.A., Lopes, A.P., Anderson, L.O., da Silva, T.F.M.R., Aragão, L.E.O.C., 2019. Translating fire impacts in Southwestern Amazonia into economic costs. Remote Sens. 11 https://doi.org/10.3390/rs11070764.

Catry, F.X., Rego, F.C., Bação, F.L., Moreira, F., 2009. Modeling and mapping wildfire ignition risk in Portugal. Int. J. Wildl. Fire 18, 921–931. https://doi.org/10.1071/WF07123.

Chen, F., Du, Y., Niu, S., Zhao, J., 2015. Modeling forest lightning fire occurrence in the Daxinganling mountains of Northeastern China with MAXENT. Forests 6, 1422–1438. https://doi.org/10.3390/f6051422.

Christian, H.J., Blakeslee, R.J., Boccippio, D.J., Boeck, W.L., Buechler, D.E., Driscoll, K. T., Goodman, S.J., Hall, J.M., Koshak, W.J., Mach, D.M., Stewart, M.F.G., 2003. Global frequency and distribution of lightning as observed from space by the optical transient detector. J. Geophys. Res. Atmos. 108.

Clarke, H., Gibson, R., Cirulis, B., Bradstock, R.A., Penman, T.D., 2019. Developing and testing models of the drivers of anthropogenic and lightning-caused wildfire ignitions in south-eastern Australia. J. Environ. Manage. 235, 34–41. https://doi.org/10.1016/j.jenvman.2019.01.055.

Collins, L., Bennett, A.F., Leonard, S.W.J., Penman, T.D., 2019. Wildfire refugia in forests: Severe fire weather and drought mute the influence of topography and fuel age. Glob. Chang. Biol. 25, 3829–3843. https://doi.org/10.1111/gcb.14735.

CONAF, 2015. Available at: http://www.conaf.cl/incendios-forestales/incendios-forestales-en-chile/. Acesses 07 August 2020.

Dowdy, A.J., 2020. Climatology of thunderstorms, convective rainfall and dry lightning environments in Australia. Clim. Dyn. 54, 3041–3052. https://doi.org/10.1007/s00382-020-05167-9.

Dowdy, A.J., Mills, G.A., 2012. Atmospheric and fuel moisture characteristics associated with lightning-attributed fires. J. Appl. Meteorol. Climatol. 51, 2025–2037. https://doi.org/10.1175/JAMC-D-11-0219.1.

Dowdy, A.J., Mills, G.A., 2009. Atmospheric states associated with the ignition of lightning-attributed fires, CAWCR Technical Report No. 019.

Egloff, B., 2017. Lightning strikes: rethinking the nexus between Australian Indigenous land management and natural forces. Aust. For. 80, 275–285. https://doi.org/10.1080/00049158.2017.1395199.

Elia, M., Giannico, V., Lafortezza, R., Sanesi, G., 2019. Modeling fire ignition patterns in Mediterranean urban interfaces. Stoch. Environ. Res. Risk Assess. 33, 169–181. https://doi.org/10.1007/s00477-018-1558-5.

Fernandes, W.A., Pinto, I.R., Pinto, J.r.O., Longo, K.M., Freitas, S.R., 2006. New findings about the influence of smoke from fires on the cloud-to-ground lightning characteristics in the Amazon region. Geophys Res Lett 33, 4–7.

Fischer, R., Taubert, F., Müller, M.S., Groeneveld, J., Lehmann, S., Wiegand, T., Huth, A., 2021. Accelerated forest fragmentation leads to critical increase in tropical forest edge area. Science advances 7 (37), eabg7012.

Fonseca, M.G., Alves, L.M., Aguiar, A.P.D., Arai, E., Anderson, L.O., Rosan, T.M., Shimabukuro, Y.E., de Aragão, L.E.O.e.C., 2019. Effects of climate and land-use change scenarios on fire probability during the 21st century in the Brazilian Amazon. Glob. Chang. Biol. 25, 2931–2946. https://doi.org/10.1111/gcb.14709.

França, H., Pereira, A., Pinto, J.R.O., Fernandes, W.A., Gomez, R.P.S., 2004. Ocorrências de raios e queimadas naturais no Parque Nacional de Emas, GO, na estação chuvosa de 2002-2003. In: Congresso Brasileiro de unidades de conservação, pp. 417–425. Curitiba. Anais v. 1.

Fuquay, D.M., Baughman, R.G., Taylor, A.R., Hawe, R.G., 1967. Characteristics of seven lightning discharges that caused forest fires. J. Geophys. Res. 72, 6371–6373. https://doi.org/10.1029/JZ072i024p06371.

Gannon, C.S., Steinberg, N.C., 2021. A global assessment of wildfire potential under climate change utilizing Keetch-Byram drought index and land cover classifications. Environ. Res. Commun. 3 (3), 035002.

G1, 2017. Bombeiros registram 44 ocorrências de incêndio ambiental no domingo (3) em Rio Branco. Available at: https://g1.globo.com/ac/acre/noticia/bombeiros-registram-44-ocorrencias-de-incendio-ambiental-no-domingo-3-em-rio-branco.ghtml. Acesses 07 August 2020.

Gadelha, A.N., Coelho, V.H.R., Xavier, A.C., Barbosa, L.R., Melo, D.C.D., Xuan, Y., Huffman, G.J., Petersen, W.A., Almeida, C.das N., 2019. Grid box-level evaluation of IMERG over Brazil at various space and time scales. Atmos. Res. 218, 231–244. 10.1016/j.atmosres.2018.12.001.

Ganteaume, A., Camia, A., Jappiot, M., San-Miguel-Ayanz, J., Long-Fournel, M., Lampin, C., 2013. A review of the main driving factors of forest fire ignition over

Europe. Environ. Manage. 51, 651–662. https://doi.org/10.1007/s00267-012-9961-z.
Giglio, L., Csiszar, I., Justice, C.O, 2006. Global distribution and seasonality of active fires as observed with the Terra and Aqua Moderate Resolution Imaging Spectroradiometer (MODIS) sensors. Journal of geophysical research: Biogeosciences 111 (G2).
Giglio, L., Schroeder, W., Justice, C.O., 2016. The collection 6 MODIS active fire detection algorithm and fire products. Remote Sens. Environ. 178, 31–41. https://doi.org/10.1016/j.rse.2016.02.054.
Hennermann, K., Berrisford, P., 2017. Era5 data documentation. Copernicus knowledge base.
Huffman, G.J., Bolvin, D.T., Nelkin, E.J., Stocker, E.F., Tan, J., 2019. V06 IMERG release notes. NASA/GSFC, Greenbelt, MD, USA.
INMET, 2020. Available at: https://clima.inmet.gov.br/NormaisClimatologicas/1961-1990/precipitacao_acumulada_mensal_anual. Acesses 07 August 2020.
INPE, 2021a. Annual estimates of burned areas. Available at www.inpe.br/queimadas/aq1km/. Acces on 08/June/2021.
INPE, 2021b. Database of wildfires detected by satellites. https://www.inpe.br/queimadas/bdqueimadas. Access on 08/June/2021.
IPCC, 2014. Climate change 2014: Mitigation of climate change. Contribution of Working Group III to the Fifth Assessment Report of the Intergovernmental Panel on Climate Change. Cambridge University Press, Cambridge UK; New York, USA.
Jolly, W.M., Cochrane, M.A., Freeborn, P.H., Holden, Z.A., Brown, T.J., Williamson, G.J., Bowman, D.M.J.S., 2015. Climate-induced variations in global wildfire danger from 1979 to 2013. Nat. Commun. 6, 1–11. https://doi.org/10.1038/ncomms8537.
Justino, F., Bromwich, D., Wilson, A., da Silva, A.S., Avila-Diaz, A., Fernandez, A., Rodrigues, J.M., 2021. Estimates of temporal-spatial variability of wildfire danger across the Pan-Arctic and extra-tropics. Environ. Res. Lett.
Kar, S.K., Liou, Y.A., 2019. Influence of land use and land cover change on the formation of local lightning. Remote Sens. 11 https://doi.org/10.3390/rs11040407.
Kganyago, M., Shikwambana, L., 2020. Assessment of the characteristics of recent major wildfires in the USA, Australia and Brazil in 2018–2019 using multi-source satellite products. Remote Sensing 12 (11), 1803.
Krause, A., Kloster, S., Wilkenskjeld, S., Paeth, H., 2014. The sensitivity of global wildfires to simulated past, present, and future lightning frequency. J. Geophys. Res. Biogeosci. 119, 312–322. https://doi.org/10.1002/2013JG002502.
Laris, P., Jacobs, R., Koné, M., Dembélé, F., Rodrigue, C.M., 2020. Determinants of fire intensity in working landscapes of an African savanna. Fire Ecol. 16 (1), 1–16.
Larjavaara, M., Pennanen, J., Tuomi, T.J., 2005. Lightning that ignites forest fires in Finland. Agric. For. Meteorol. 132, 171–180. https://doi.org/10.1016/j.agrformet.2005.07.005.
Leal Filho, W., Azeiteiro, U.M., Salvia, A.L., Libonati, R., 2021. Fire in paradise: why the Pantanal is burning. Environ. Sci. Pol. 123, 31–34. https://doi.org/10.1016/j.envsci.2021.05.005.
Llauca, H., Lavado-Casimiro, W., León, K., Jimenez, J., Traverso, K., Rau, P., 2021. Assessing near real-time satellite precipitation products for flood simulations at sub-daily scales in a sparsely gauged watershed in Peruvian Andes. Remote Sensing 13 (4), 826.
Li, Y., Mickley, L., Liu, P., Kaplan, J., 2020. Trends and spatial shifts in lightning fires and smoke concentrations in response to 21st century climate over the forests of the Western United States. Atmos. Chem. Phys. 1–26 https://doi.org/10.5194/acp-2020-80.
Liu, Z., Yang, J., Chang, Y., Weisberg, P.J., He, H.S., 2012. Spatial patterns and drivers of fire occurrence and its future trend under climate change in a boreal forest of Northeast China. Global Change Biol. 18 (6), 2041–2056.
Luo, R., Hui, D., Miao, N., Liang, C., Wells, N., 2017. Global relationship of fire occurrence and fire intensity: A test of intermediate fire occurrence-intensity hypothesis. J. Geophys. Res.: Biogeosci. 122 (5), 1123–1136.
Macário, L., 2014. Ação humana é responsável por 99% das queimadas no Brasil, diz especialista. Available at. https://www.camara.leg.br/noticias/439737-ACAO-HUMANA-E-RESPONSAVEL-POR-99-DAS-QUEIMADAS-NO-BRASIL,-DIZ-ESPECIALISTA. Câmara dos Deputados. Acessed 07 August 2020.
MacNamara, B.R., Schultz, C.J., Fuelberg, H.E., 2020. Flash characteristics and precipitation metrics of western U.S. lightning-initiated wildfires from 2017. Fire 3, 5. https://doi.org/10.3390/fire3010005.
Mariani, M., Holz, A., Veblen, T.T., Williamson, G., Fletcher, M.S., Bowman, D.M.J.S., 2018. Climate change amplifications of climate-fire teleconnections in the southern hemisphere. Geophys. Res. Lett. 45, 5071–5081. https://doi.org/10.1029/2018GL078294.
Martínez, J., Vega-Garcia, C., Chuvieco, E., 2009. Human-caused wildfire risk rating for prevention planning in Spain. J. Environ. Manage. 90, 1241–1252. https://doi.org/10.1016/j.jenvman.2008.07.005.
Moazami, S., Najafi, M.R., 2021. A comprehensive evaluation of GPM-IMERG V06 and MRMS with hourly ground-based precipitation observations across Canada. J. Hydrol. 594, 125929.
Moris, J.V., Conedera, M., Nisi, L., Bernardi, M., Cesti, G., Pezzatti, G.B., 2020. Lightning-caused fires in the Alps: identifying the igniting strokes. Agric. For. Meteorol. 290, 107990 https://doi.org/10.1016/j.agrformet.2020.107990.
Naccarato, K.P., Pinto, O., 2009. Improvements in the detection efficiency model for the Brazilian lightning detection network (BrasilDAT). Atmos. Res. 91, 546–563. https://doi.org/10.1016/j.atmosres.2008.06.019.
Naccarato, K.P., Pinto Jr, O., Pinto, I.R.C.A., 2003. Evidence of thermal and aerosol effects on the cloud-to-ground lightning density and polarity over large urban areas of Southeastern Brazil. Geophys. Res. Lett. 30 (13).
Naccarato, K.P., Saraiva, A.C.V., Saba, M.M.F., Schumann, C., Pinto Jr, O., 2012. First performance analysis of BrasilDAT total lightning network in southeastern Brazil. In: International Conference On Grounding And Earthing (GROUND'2012). Bonito, Brazil.
Nadeem, K., Taylor, S.W., Woolford, D.G., Dean, C.B., 2019. Mesoscale spatiotemporal predictive models of daily human- and lightning-caused wildland fire occurrence in British Columbia. Int. J. Wildl. Fire 29, 11–27. https://doi.org/10.1071/WF19058.
Nampak, H., Love, P., Fox-Hughes, P., Watson, C., Aryal, J., Harris, R.M.B., 2021. Characterizing spatial and temporal variability of lightning activity associated with wildfire over Tasmania. Australia. Fire 4, 10. https://doi.org/10.3390/fire4010010.
Nauslar, N., Brown, R., Wallmann, D., 2008. A forecast procedure for dry lightning potential. Ams. Confex. Com. 1, 200–214.
Nepal, B., Shrestha, D., Sharma, S., Shrestha, M.S., Aryal, D., Shrestha, N., 2021. Assessment of GPM-era satellite products'(IMERG and GSMaP) ability to detect precipitation extremes over mountainous country Nepal. Atmosphere 12 (2), 254.
Ojerio, R., Moseley, C., Lynn, K., Bania, N., 2011. Limited involvement of socially vulnerable populations in federal programs to mitigate wildfire risk in Arizona. Nat. Hazards Rev. 12, 28–36. https://doi.org/10.1061/(ASCE)NH.1527-6996.0000027.
Oliveira, S.L., Maier, S.W., Pereira, J.M., Russell-Smith, J., 2015. Seasonal differences in fire activity and intensity in tropical savannas of northern Australia using satellite measurements of fire radiative power. Int. J. Wildl. Fire 24 (2), 249–260.
Pausas, J.G., Keeley, J.E., 2021. Wildfires and global change. Front. Ecol. Environ.
Pereira, A., França, H., 2005. Identificação de queimadas naturais ocorridas no período chuvoso de 2003-2004 no Parque Nacional das Emas, Brasil, por meio de imagens dos sensores do satélite CBERS-2. XI I Simpósio Bras. Sensoriamento Remoto 3245–3252.
Pineda, N., Montanyà, J., van der Velde, O.A., 2014. Characteristics of lightning related to wildfire ignitions in Catalonia. Atmos. Res. 135–136, 380–387. https://doi.org/10.1016/j.atmosres.2012.07.011.
Pinto Jr., O., Pinto, I.R.C.A., 2018. BrasilDAT dataset : combining data from different lightning locating systems to obtain more precise lightning information. In: 25th Int. Light. Detect. Conf. 7th Int. Light. Meteorol. Conf. March, p. 12. -1.
Pivello, V.R., 2011. The use of fire in the cerrado and Amazonian rainforests of Brazil: past and present. Fire Ecol. 7, 24–39. https://doi.org/10.4996/fireecology.0701024.
Price, C., 2009. Will a drier climate result in more lightning? Atmos. Res. 91, 479–484. https://doi.org/10.1016/j.atmosres.2008.05.016.
Rakov, V.A., Uman, M.A., 2003. Lightning: Physics and Effects, 1st Ed. Cambridge University Press, Cambridge. https://doi.org/10.1017/CBO9781107340886.
Ramos-Neto, M.B., Pivello, V.R., 2000. Lightning fires in a Brazilian Savanna National Park: rethinking management strategies. Environ. Manage. 26, 675–684. https://doi.org/10.1007/s002670010124.
Read, N., Duff, T.J., Taylor, P.G., 2018. A lightning-caused wildfire ignition forecasting model for operational use. Agric. For. Meteorol. 253–254, 233–246. https://doi.org/10.1016/j.agrformet.2018.01.037.
Reeve, N., Toumi, R., 1999. Lightning activity as an indicator of climate change. Q. J. R. Meteorol. Soc. 125, 893–903. https://doi.org/10.1256/smsqj.55506.
Rodman, K.C., Veblen, T.T., Saraceni, S., Chapman, T.B., 2019. Wildfire activity and land use drove 20th-century changes in forest cover in the Colorado front range. Ecosphere 10. https://doi.org/10.1002/ecs2.2594.
Rodríguez-Pérez, J.R., Ordóñez, C., Roca-Pardiñas, J., Vecín-Arias, D., Castedo-Dorado, F., 2020. Evaluating lightning-caused fire occurrence using spatial generalized additive models: a case study in Central Spain. Risk Anal. 40, 1418–1437. https://doi.org/10.1111/risa.13488.
Rojas, Y., Minder, J.R., Campbell, L.S., Massmann, A., Garreaud, R., 2021. Assessment of GPM IMERG satellite precipitation estimation and its dependence on microphysical rain regimes over the mountains of South-Central Chile. Atmospheric Res. 253, 105454.
Romps, D.M., Seeley, J.T., Vollaro, D., Molinari, J., 2014. Projected increase in lightning strikes in the United States due to global warming. Science (80-.) 346, 851–854. https://doi.org/10.1126/science.1259100.
Rorig, M.L., Ferguson, S.A., 2002. The 2000 fire season: Lightning-caused fires. J. Appl. Meteorol. 41 (7), 786–791.
Rozante, J.R., Vila, D.A., Barboza Chiquetto, J., Fernandes, A.D.A., Souza Alvim, D., 2018. Evaluation of TRMM/GPM blended daily products over Brazil. Remote Sensing 10 (6), 882.
Saba, M.M.F., Ballarotti, M.G., Pinto, J.R., O., 2006a. Negative cloud-to-ground lightning properties from high-speed video observations. J. Geophys. Res., Estados Unidos v. 111 (n. D03101), D03101.
Saba, M.M.F., PINTO, J.R.O., Ballarotti, M.G., 2006b. Relation between lightning return stroke peak current and following continuing current. Geophys. Res. Lett., Washington, EUA v. 33 (n. L23807), L23807.
Saba, M.M., Schulz, W., Warner, T.A., Campos, L.Z., Schumann, C., Krider, E.P., Cummins, K.L., Orville, R.E., 2010. High-speed video observations of positive lightning flashes to ground. J. Geophys. Res. 115, D24201. https://doi.org/10.1029/2010JD014330.
Sannigrahi, S., Pilla, F., Basu, B., Basu, A.S., Sarkar, K., Chakraborti, S., Roy, P.S, 2020. Examining the effects of forest fire on terrestrial carbon emission and ecosystem production in India using remote sensing approaches. Sci. Total Environ. 725, 138331.
Santos, J., 2004. Estatísticas de incêndios florestais em áreas protegidas no período de 1998 a 2002. 76 f. Setor de Ciências Agrárias, Universidade Federal do Paraná, Curitiba.
Saraiva, A.C.V., Saba, M.M.F., Pinto, O., Cummins, K.L., Krider, E.P., Campos, L.Z.S, 2010. A comparative study of negative cloud-to-ground lightning characteristics in São Paulo (Brazil) and Arizona (United States) based on high-speed video observations. J. Geophys. Res. v. 115, D11102.

Schoennagel, T., Veblen, T.T., Romme, W.H., 10.1641/0006-3568(2004)054[0661:tioffa]2.0.co;2, 2004. The interaction of fire, fuels, and climate across rocky mountain forests. Bioscience 54, 661.

Schroeder, W., Oliva, P., Giglio, L., Csiszar, I.A., 2014. The New VIIRS 375m active fire detection data product: algorithm description and initial assessment. Remote Sens. Environ. 143, 85–96. https://doi.org/10.1016/j.rse.2013.12.008.

Schultz, C.J., Nauslar, N.J., Wachter, J.B., Hain, C.R., Bell, J.R., 2019. Spatial, temporal and electrical characteristics of lightning in reported lightning-initiated wildfire events. Fire 2, 18. https://doi.org/10.3390/fire2020018.

Schumacher, V., Setzer, A., 2021. Relação entre queimadas e relâmpagos no Parque Nacional das Emas. In: Setzer, A., Ferreira, N.J. (Eds.), Queimadas e incêndios florestais: mediante monitoramento orbital, 2021. Oficina de Textos, São Paulo, pp. 118–130 cap. 5.

Seity, Y., Soula, S., Sauvageot, H., 2001. Lightning and precipitation relationship in coastal thunderstorms. J. Geophys. Res.: Atmospheres 106 (D19), 22801–22816.

Sevinc, V., Kucuk, O., Goltas, M., 2020. A Bayesian network model for prediction and analysis of possible forest fire causes. Forest Ecol. Manage. 457, 117723.

Shi, Z., Tan, Y., Liu, Y., Liu, J., Lin, X., Wang, M., Luan, J., 2018. Effects of relative humidity on electrification and lightning discharges in thunderstorms. Terrestrial, Atmosp. Oceanic Sci. 29 (6).

Shikwambana, L., Kganyago, M., 2021. Observations of emissions and the influence of meteorological conditions during wildfires: a case study in the USA, Brazil, and Australia during the 2018/19. Period. Atmosphere 12 (1), 11.

Silva, A.S., Justino, F., Setzer, A.W., Avila-Diaz, A., 2021. Vegetation fire activity and the Potential Fire Index (PFIv2) performance in the last two decades (2001–2016). Int. J. Climatol. 41, E78–E92.

Silva Junior, C.H., Aragão, L.E., Fonseca, M.G., Almeida, C.T., Vedovato, L.B., Anderson, L.O., 2018. Deforestation-induced fragmentation increases forest fire occurrence in central Brazilian Amazonia. Forests 9 (6), 305.

Silva, P.S., Nogueira, J., Rodrigues, J.A., Santos, F.L., Pereira, J.M., DaCamara, C.C., Libonati, R., 2021. Putting fire on the map of Brazilian savanna ecoregions. J. Environ. Manage. 296, 113098.

Singh, M.S., Kuang, Z., Maloney, E.D., Hannah, W.M., Wolding, B.O., 2017. Increasing potential for intense tropical and subtropical thunderstorms under global warming. Proc. Natl. Acad. Sci. U. S. A. 114, 11657–11662. https://doi.org/10.1073/pnas.1707603114.

Siqueira, R.A.D., Vila, D.A., Afonso, J.M.D.S., 2021. The performance of the diurnal cycle of precipitation from blended satellite techniques over Brazil. Remote Sensing 13 (4), 734.

Tolentino, L., 2014. Ser humano é o maior culpado pelo aumento de incêndios florestais. Ministério do Meio Ambiente. Available at: https://www.mma.gov.br/informma/item/12310-noticia-acom-2014-08-433.html. Acesses 07 August 2020.

Úbeda, X., Sarricolea, P., 2016. Wildfires in Chile: a review. Glob. Planet. Change 146, 152–161. https://doi.org/10.1016/j.gloplacha.2016.10.004.

Vant-Hull, B., Thompson, T., Koshak, W., 2018. Optimizing precipitation thresholds for best correlation between dry lightning and wildfires. J. Geophys. Res. Atmos. 123, 2628–2639. https://doi.org/10.1002/2017JD027639.

Veraverbeke, S., Rogers, B.M., Goulden, M.L., Jandt, R.R., Miller, C.E., Wiggins, E.B., Randerson, J.T., 2017. Lightning as a major driver of recent large fire years in North American boreal forests. Nat. Clim. Chang. 7, 529–534. https://doi.org/10.1038/nclimate3329.

Wang, H., Shi, Z., Wang, X., Tan, Y., Wang, H., Li, L., Lin, X., 2021. Cloud-to-ground lightning response to aerosol over air-polluted urban areas in China. Remote Sensing 13 (13), 2600.

Wang, Y., Anderson, K.R., 2010. An evaluation of spatial and temporal patterns of lightning- and human-caused forest fires in Alberta, Canada, 1980-2007. Int. J. Wildl. Fire 19, 1059–1072. https://doi.org/10.1071/WF09085.

Werf, G.R., Randerson, J.T., Giglio, L., Van Leeuwen, T.T., Chen, Y., Rogers, B.M., Mu, M., Van Marle, M.J.E., Morton, D.C., Collatz, G.J., Yokelson, R.J., Kasibhatla, P. S., 2017. Global fire emissions estimates during 1997-2016. Earth Syst. Sci. Data 9, 697–720. https://doi.org/10.5194/essd-9-697-2017.

Westerling, A.L., Hidalgo, H.G., Cayan, D.R., Swetnam, T.W., 2006. Warming and earlier spring increase Western U.S. forest wildfire activity. Science 313, 940–943. https://doi.org/10.1126/science.1128834.

Williams, E., Mushtak, V., Rosenfeld, D., Goodman, S., Boccippio, D., 2005. Thermodynamic conditions favorable to superlative thunderstorm updraft, mixed phase microphysics and lightning flash rate. Atmos. Res. 76, 288–306. 10.1016/j.atmosres.2004.11.009.

WMO-World Meteorological Organization, 1994. Guide to hydrological practices, data acquisition and processing, analysis, forecasting and other applications. Geneva, Switzerland.

Wotton, B.M., Martell, D.L., 2005. A lightning fire occurrence model for Ontario. Can. J. For. Res. 35, 1389–1401. https://doi.org/10.1139/x05-071.

Ye, T., Wang, Y., Guo, Z., Li, Y., 2017. Factor contribution to fire occurrence, size, & burn probability in a subtropical coniferous forest in East China. PLoS One 12, 1–18. https://doi.org/10.1371/journal.pone.0172110.

Zepka, G.S., Pinto, O., Saraiva, A.C.V., 2014. Lightning forecasting in southeastern Brazil using the WRF model. Atmos. Res. 135–136, 344–362. https://doi.org/10.1016/j.atmosres.2013.01.008.

Zhu, Y., Rakov, V.A., Tran, M.D., Stock, M.G., Heckman, S., Liu, C., Hare, B.M., 2017. Evaluation of ENTLN performance characteristics based on the ground truth natural and rocket-triggered lightning data acquired in Florida. J. Geophys. Res.: Atmospheres 122, 9858–9866. https://doi.org/10.1002/2017JD027270.

Zhu, Y., Rakov, V.A., Tran, M.D., Nag, A., 2016. A study of national lightning detection network responses to natural lightning based on ground truth data acquired at LOG with emphasis on cloud discharge activity. J. Geophys. Res. Atmos. 121, 14651–14660. https://doi.org/10.1002/2016JD025574.

Zhou, C., Gao, W., Hu, J., Du, L., Du, L., 2021. Capability of IMERG V6 early, late, and final precipitation products for monitoring extreme precipitation events. Remote Sensing 13 (4), 689.